Surface Geophysical Exploration of C Tank Farm at the Hanford Site

M. Levitt and D. Rucker hydroGEOPHYSICS, Inc.
C. Henderson and K. Williams Columbia Energy & Environmental Services
Richland, WA 99352
U.S. Department of Energy Contract DE-AC27-99RL14047

EDT/ECN:	DRF	UC:	
Cost Center:		Charge Code:	
B&R Code:		Total Pages:	57

Key Words: Surface geophysical exploration, C Tank Farm, electrical resistivity, characterization

Abstract: This report presents the results of an investigation at C tank farm at the Hanford Site for subsurface contamination using electrical resistivity methods. Geophysical exploration activities included collecting and analyzing resisitivity data using shallow surface electrodes, wells, and buried electrodes.

TRADEMARK DISCLAIMER. Reference herein to any specific commercial product, process, or service by trade name, trademark, manufacturer, or otherwise, does not necessarily constitute or imply its endorsement, recommendation, or favoring by the United States Government or any agency thereof or its contractors or subcontractors.

Printed in the United States of America. To obtain copies of this document, contact: Document Control Services, P.O. Box 950, Mailstop H6-08, Richland WA 99352, Phone (509) 372-2420; Fax (509) 376-4989.

MAR 27 2007
DATE:
STA: 15
HANFORD RELEASE
ID: 65

Release Approval — Date 03/27/07

Release Stamp

Approved For Public Release

RPP-RPT-31558, Revision 0

Surface Geophysical Exploration of C Tank Farm at the Hanford Site

M. Levitt
D. Rucker
hydroGEOPHYSICS, Inc.

C. Henderson
K. Williams
Columbia Energy & Environmental Services, Inc.

Date Published
February 2007

CH2MHILL
Hanford Group, Inc.
Post Office Box 1500
Richland, Washington

Prepared for the U.S. Department of Energy
Office of River Protection

Contract # DE-AC27-99RL14047, Modification M030

EXECUTIVE SUMMARY

This report documents the results of preliminary surface geophysical exploration (SGE) activities performed between August and December 2006 for the C tank farm. The C tank farm is located in the 200 East Area at the U.S. Department of Energy Hanford Site in Washington State. The objective of the preliminary investigation was to collect and analyze an initial set of resistivity data to identify low-resistivity regions that could be correlated to soil inventory records. The resistivity data will be used to aid in selection of locations for conventional sampling and analysis.

The preliminary geophysical investigation was performed by collecting resistivity data using 69 drywells within the tank farm, 8 monitoring boreholes (e.g., groundwater wells) outside the tank farm, 1 buried electrode recently installed in the west end of the tank farm, and 4 surface electrode arrays outside of the farm. The 4 surface electrode arrays were located outside of the farm and were oriented parallel to the perimeter of the tank farm fenceline. The 4 surface arrays provided limited coverage, but were deployed in an effort to investigate areas near the tank farm fenceline for targeting future characterization activities. The limited coverage data collection strategy was used to collect data in support of near-term planned characterization while limiting resources required for multiple tank farm entries. This deployment is similar to that performed at U tank farm (*Surface Geophysical Exploration of U Tank Farm at the Hanford Site*[1]).

The 4 surface electrode arrays did not provide for collection of surface data throughout the tank farm in the same manner as recent SGE deployments at S tank farm (*Surface Geophysical Exploration of S Tank Farm at the Hanford Site*[2]) and T tank farm (*Surface Geophysical Exploration of T Tank Farm* [3]) where surface electrode arrays were deployed throughout the tank farms. The C tank farm SGE data that used surface electrodes, including surface-to-surface (STS) and well-to-surface (WTS), were inferior to those obtained for the S tank farm SGE due to the limited coverage and interferences from metallic infrastructure and electrical noise. Thus, the three-dimensional representations including surface electrode data produced unsatisfactory results.

Like U-farm, analysis of C tank farm well-to-well (WTW) results demonstrated that WTW resistivity data have the capability to identify and delineate contaminant plume features within and around tank farms that contain metallic infrastructure such as pipes, tanks, diversion boxes, and utilities. Resistivity data collected via the 69 drywells used in a WTW resistivity inversion can be used to locate and map areas of low resistivity. Areas of low resistivity are most likely associated with increased soil moisture or inorganic salt concentration. Additionally, the investigation identified specific areas of low-resistivity values within the C tank farm that can be correlated with current interpretations of historical data. Specifically, the WTW data indicate a low-resistivity region near tanks C-104 and C-105, along with a smaller low-resistivity zone near C-108 (Figure ES-1).

---

[1] RPP-RPT-31557, 2006, *Surface Geophysical Exploration of U Tank Farm at the Hanford Site*, Rev. 0, CH2M HILL Hanford Group, Inc., Richland, Washington.

[2] RPP-RPT-30976, 2006, *Surface Geophysical Exploration of S Tank Farm at the Hanford Site*, Rev. 0, CH2M HILL Hanford Group, Inc., Richland, Washington.

[3] RPP-RPT-28955, 2006, *Surface Geophysical Exploration of T Tank Farm*, Rev. 0, CH2M HILL Hanford Group, Inc., Richland, Washington.

Figure ES-1. Well-to-Well Inversion Results with Drywells Only.

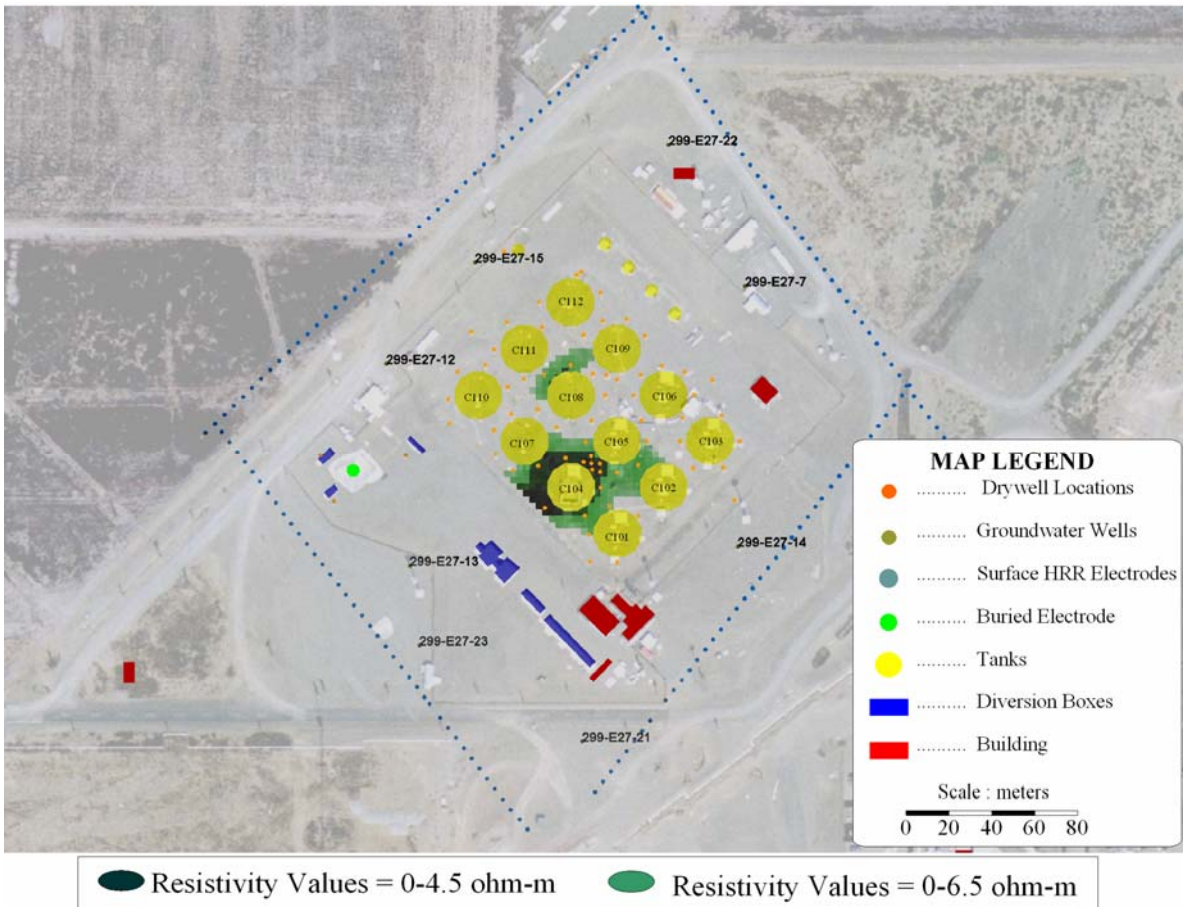

The remaining resistivity data sets (WTS, STS, and WTW with groundwater wells) provided limited value due to spatial coverage, data density, or electrical signal quality problems. For example, the surface lines were placed on the perimeter of the C tank farm with no lines running through the center of the farm. The distance between the drywells, located inside the tank farm fence, and the surface lines outside the fence, was too great to obtain reliable inversion results between the two areas. Additionally, the large distance between the two datasets caused modeling limitations that forced the modeling domain to be divided into smaller subsets. Lastly, it appears that some of the surface data suffered from interferences caused by near surface metallic infrastructure that renders plume interpretation unreliable.

The single-depth electrode did not provide additional supporting data due to its placement, which was beyond the WTW modeling area, and the limited quantity of data provided by a single electrode. However, sufficient data were acquired to verify that the deployment technique, used to install the depth electrode, produces reliable data. Results from forward modeling, conducted as part of the T farm SGE project[3], showed a significant increase in vertical resolution when several depth electrodes are deployed in dispersed locations throughout the WTW modeling area.

Several recommendations are suggested to improve the data acquisition, data quality, and data coverage of future SGE efforts in and around the C tank farm:

1. It is strongly recommended that a full data set inversion be performed when the inversion software upgrade is completed. All inversion results, with the exception of WTW with the drywells only, suffered as a result of the inversion software and hardware limitations that forced modelers to break data sets into smaller fractions of the total data population. The complexity and large spatial area of the C farm project site could not be adequately modeled using current inversion software and hardware. However, results of the individual modeling subsets suggest that good information could be achieved if all electrode data sets are inverted as a single model.

2. All inversion results that used surface data suffered as a result of the reduced electrode deployment, which consisted of four orthogonal lines surrounding the C tank farm perimeter. Inversion results for this SGE effort demonstrate that surface data are only valuable when deployed with sufficient resolution and geometry. Future SGE efforts should be deployed with sufficient line and electrode spacing to adequately resolve the spatial and vertical location of observed resistivity anomalies. At a minimum, surface electrodes should be deployed along equally spaced orthogonal lines, similar to previous work at T and S tank farms.

3. If limited scope SGE deployments are performed, the investigation should be limited to WTW data collection.

4. Vertical resolution is relatively low (compared to lateral resolution) for the surface resistivity data collection and non-existent for WTW resistivity. It is recommended that future SGE deployments include as many subsurface point electrodes as possible that are located within the central monitoring well area. An additional enhancement would be to deploy several depth electrodes along each borehole in order to construct an electrical resistivity tomography array. Forward modeling demonstrated a significant improvement in vertical resolution using depth electrode data.

5. Develop a strategy to increase confidence in the SGE results through confirmatory vadose zone sediment and pore water sampling analysis of key inorganic constituents in the vadose zone.

TABLE OF CONTENTS

1.0 INTRODUCTION 1
- 1.1 SCOPE 1
- 1.2 OBJECTIVES 1
- 1.3 REPORT LAYOUT 1

2.0 BACKGROUND 2
- 2.1 TANK CONTENTS 7
- 2.2 FLUID DISCHARGE AT OR NEAR C TANK FARM 8

3.0 DATA COLLECTION 9
- 3.1 SURVEY AREA AND COVERAGE 9
  - 3.1.1 Surface-to-Surface Data Acquisition 13
  - 3.1.2 Well-to-Surface and Buried Electrode-to-Surface Data Acquisition 16
  - 3.1.3 Well-to-Well and Well-to-Buried Electrode Data Acquisition 16
- 3.2 INSTALLATION AND SETUP 17
  - 3.2.1 Installation of Remote Reference Arrays 19
  - 3.2.2 Permanent Surface Electrodes 19
  - 3.2.3 Resistivity Equipment 19
  - 3.2.4 Weather Conditions 19

4.0 ANALYSIS RESULTS AND INTERPRETATION 20
- 4.1 SURFACE-TO-SURFACE ELECTRICAL RESISTIVITY INVERSION 21
- 4.2 WELL-TO-WELL ELECTRICAL RESISTIVITY INVERSION 23
- 4.3 WELL-TO-SURFACE ELECTRICAL RESISTIVITY INVERSION 26
- 4.4 COMBINATION WELL-TO-WELL, WELL-TO-SURFACE, AND SURFACE-TO-SURFACE ELECTRICAL RESISTIVITY INVERSION 29

5.0 CONCLUSIONS 31

6.0 LIMITATIONS 33
- 6.1 MODEL DOMAIN LIMITATIONS 33
- 6.2 ISSUES AND CONCERNS ASSOCIATED WITH INTERPRETATION 37

7.0 RECOMMENDATIONS 38

8.0 REFERENCES 39

LIST OF APPENDICES

A C TANK FARM SURFACE GEOPHYSICAL EXPLORATION FIGURES ..... A-i

LIST OF FIGURES

1. C Tank Farm Complex Base Map. 3
2. Typical Configuration and Dimensions of 100-Series and 200-Series Single-Shell Tanks in C Tank Farm. 4
3. Location of C Tank Farm and Surrounding Facilities. 8
4. Estimated Near Surface Fluid Discharges Summary (gallons) in C Waste Management Area. 10
5. Groundwater Nitrate Concentrations (milligrams/liter) around C Tank Farm. 11
6. Geophysical Data Collection Area Showing Location of High-Resolution Resistivity Survey Lines and Wells at C Tank Farm. 12
7. Location of Drywells and Monitoring Boreholes Used for Surface Geophysical Exploration Survey. 15
8a. Forward Pole-Pole Electrode Measurement. 17
8b. Reverse Pole-Pole Electrode Measurement. 17
9. Equipment and Setup for the Well-to-Surface Survey. 18
10. Field Worker Attaching Wire to Well. 18
11. Environmental Conditions During the Survey. 20
12. WTW Inversion Results using Drywells Only. 24
13. WTW Inversion Results using Drywell Only Data Showing Detail Around C-104. 24
14. Map of C Farm Showing WTW Inversion Modeling Domains. 25
15. Map of C Farm Showing WTS Inversion Modeling Domains. 28
16. Map of C Farm Showing Combination Inversion Modeling Domains. 30
17. Inversion Results for WTW ‘All Wells Central Domain.’ 34
18. Inversion results for WTW ‘All Wells South Domain.’ 34
19. Inversion results for WTS ‘South Domain.’ 35
20. Inversion results for WTS ‘West Domain.’ 35
21. Inversion results for WTW&STS ‘South Domain.’ 36
22. Inversion results for WTW&STS&WTS ‘South Domain.’ 36

LIST OF TABLES

1. Summary of Data Coverage. 13
2. Wells Used for Surface Geophysical Exploration Survey. 14
3. Resistivity Data Statistics for the HRR and EarthImager2D Inversion Procedures. 21
4. Comparison of WTW Inversion Results for the Individual Modeling Domains. 26
5. Comparison of WTS Inversion Results for the Individual Modeling Domains. 28
6. Comparison of WTS Final Inversion Results for the Individual Modeling Domains. 31

LIST OF TERMS

Terms

Conductivity. The ability of a material to transmit or conduct an electric impulse; reciprocal of resistivity.

Inversion. Inversion, or inverse modeling, attempts to reconstruct subsurface features from a given set of geophysical measurements, and to do so in a manner that the model response fits the observations according to some measure of error.

Petrophysical. Petrophysics pertains to the determination of physical properties of rocks through various geophysical methods including laboratory studies, borehole investigations, and/or field surveys.

Resistance. The opposition of a material to current passing through it; received voltage normalized by transmitted current.

Resistivity. A material property that is measured as its resistance to current per unit length for a uniform cross section; reciprocal of conductivity.

SuperSting R8 IP. SuperSting R8 resistivity and induced polarization meter produced by Advanced Geosciences, Inc.

Tomography. A method of producing a three-dimensional image of a volumetric object (plume) by the observation and recording of the differences in the effects on the passage of waves of energy impinging on that object.

Abbreviations and Acronyms

DOE	U.S. Department of Energy
HRR	high-resolution resistivity
PUREX	plutonium-uranium extraction
RMS	root mean square
SGE	surface geophysical exploration
STS	surface-to-surface
WTS	well-to-surface
WTW	well-to-well

1.0 INTRODUCTION

Beginning in August 2006 and ending in December 2006, a geophysical study was completed of the 241-C tank farm at the U.S. Department of Energy (DOE) Hanford Site in south central Washington State. Columbia Energy & Environmental Services, Inc. of Richland, Washington, and hydroGEOPHYSICS, Inc. of Tucson, Arizona, with support from CH2M HILL Hanford Group, Inc. conducted geophysical surveys of the C tank farm, located in the 200 East Area of the Hanford Site.

1.1 SCOPE

The scope of the geophysical surveying encompassed data acquisition using surface electrodes, borehole casings, and one buried electrode, data processing (i.e., quality assurance, quality control, data reduction, and electrical resistivity inversion modeling), and visualization (i.e., either two-dimensional contour plots of individual resistivity lines, two-dimensional contour plots of well-to-well [WTW] inversion plots, or rendered three-dimensional solid model plumes).

C tank farm data acquisition included collection of resistivity data using 4 surface geophysical exploration (SGE) lines around the perimeter of the tank farm, 77 available drywells and monitoring wells in and around the C tank farm, and one buried electrode. All surface electrodes were placed outside the tank farm fences; surface electrode lines were of sufficient length to extend the depth of investigation to groundwater. Groundwater is present at a depth of approximately 255 feet (77 meters) below ground surface.

1.2 OBJECTIVES

The main objective for this geophysical investigation was to use SGE methods to identify zones of low resistivity in the subsurface in and around the C tank farm with surface-to-surface (STS), well-to-surface (WTS), and WTW resistivity data. These data could potentially be used to aid in selection of drilling and sampling locations within the tank farm.

1.3 REPORT LAYOUT

This report is divided into seven main sections.

- **Section 1.0, Introduction** – Describes the scope and objectives of the investigation.
- **Section 2.0, Background** – Describes the setting of the C tank farm and information regarding the disposal activities in and around the tank farm.
- **Section 3.0, Data Collection** – Discusses the methodology and logistics of conducting the geophysical survey at the C tank farm.

- **Section 4.0, Analysis Results and Interpretation** – Presents the results from the surveying effort.
- **Section 5.0, Conclusions** – Provides conclusions drawn from the results, interpretations, and subsequent assessment of results.
- **Section 6.0, Issues and Concerns with Interpretation** – Discussion of problems associated with inversion modeling and interpretation of results.
- **Section 7.0, Recommendations** – Provides recommendations for improving follow-on SGE efforts.
- **Section 8.0, References** – Lists reference documents cited in the report.

2.0 BACKGROUND

The C tank farm is 1 of 12 single-shell tank farms on the Hanford Site. The C tank farm is located in the eastern portion of 200 East Area of the Hanford Site (Figure 1). The tank farm was constructed from 1943 through 1944, put into service in 1946, and is currently out of service pending final waste retrieval actions. Because of its long operational history, the C tank farm received waste generated by essentially all of the Hanford Site major chemical processing operations including bismuth phosphate fuel processing, uranium recovery, plutonium-uranium extraction (PUREX) fuel processing, and fission product recovery (RPP-14430, *Subsurface Conditions Description of the C and A-AX Waste Management Areas*). Information on the geology and hydrology of the C tank farm area can be found in RPP-23748, *Geology, Hydrogeology, Geochemistry, and Mineralogy Data Package for the Single-Shell Tank Waste Management Areas at the Hanford Site*.

The C tank farm comprises the following:

- Twelve 100-Series SSTs with a 530,000-gallon (2.0×10^6-liter) capacity (Figure 2)
- Four 200-Series SSTs with a 55,000-gallon (0.21×10^6-liter) capacity (Figure 2)
- Waste transfer lines
- Leak detection systems
- Tank ancillary equipment.

The 100-Series tanks are 75 feet (22.9 meters) in diameter and 30 feet (9 meters) tall. The tanks have a 16-foot (4.6-meter) operating depth, and an operating capacity of 530,000 gallons (2.0×10^6 liters) each. The 200-Series tanks are 20 feet (6.1 meters) in diameter and 37 feet (11.3 meters) tall from base to dome. The tanks have a 24-foot (7.3-meter) operating depth and an operating capacity of 55,000 gallons (0.21×10^6 liters) each. Typical tank configuration and dimensions are shown in Figure 2.

Figure 1. C Tank Farm Complex Base Map.

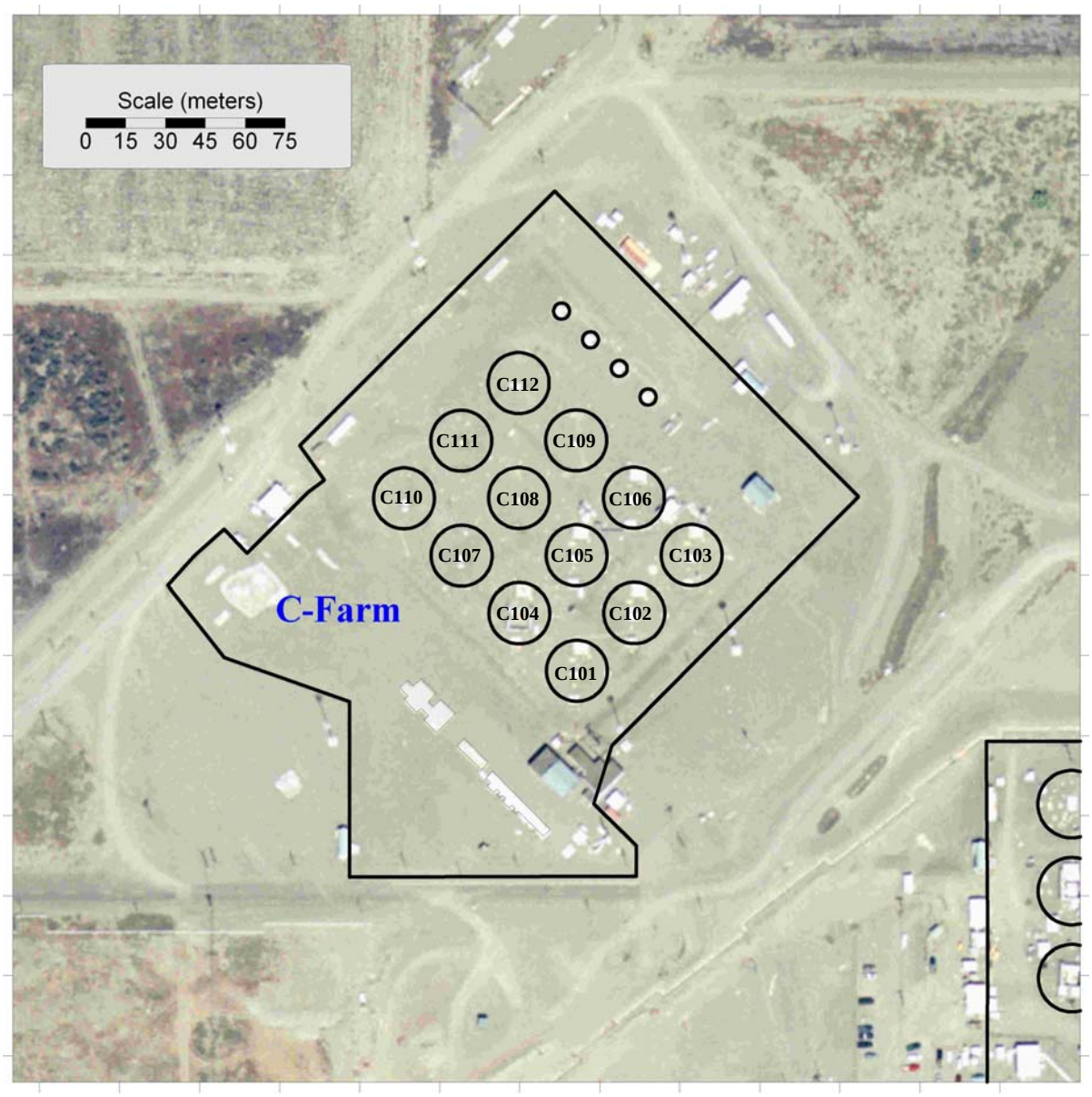

Figure 2. Typical Configuration and Dimensions of 100-Series and 200-Series Single-Shell Tanks in C Tank Farm.

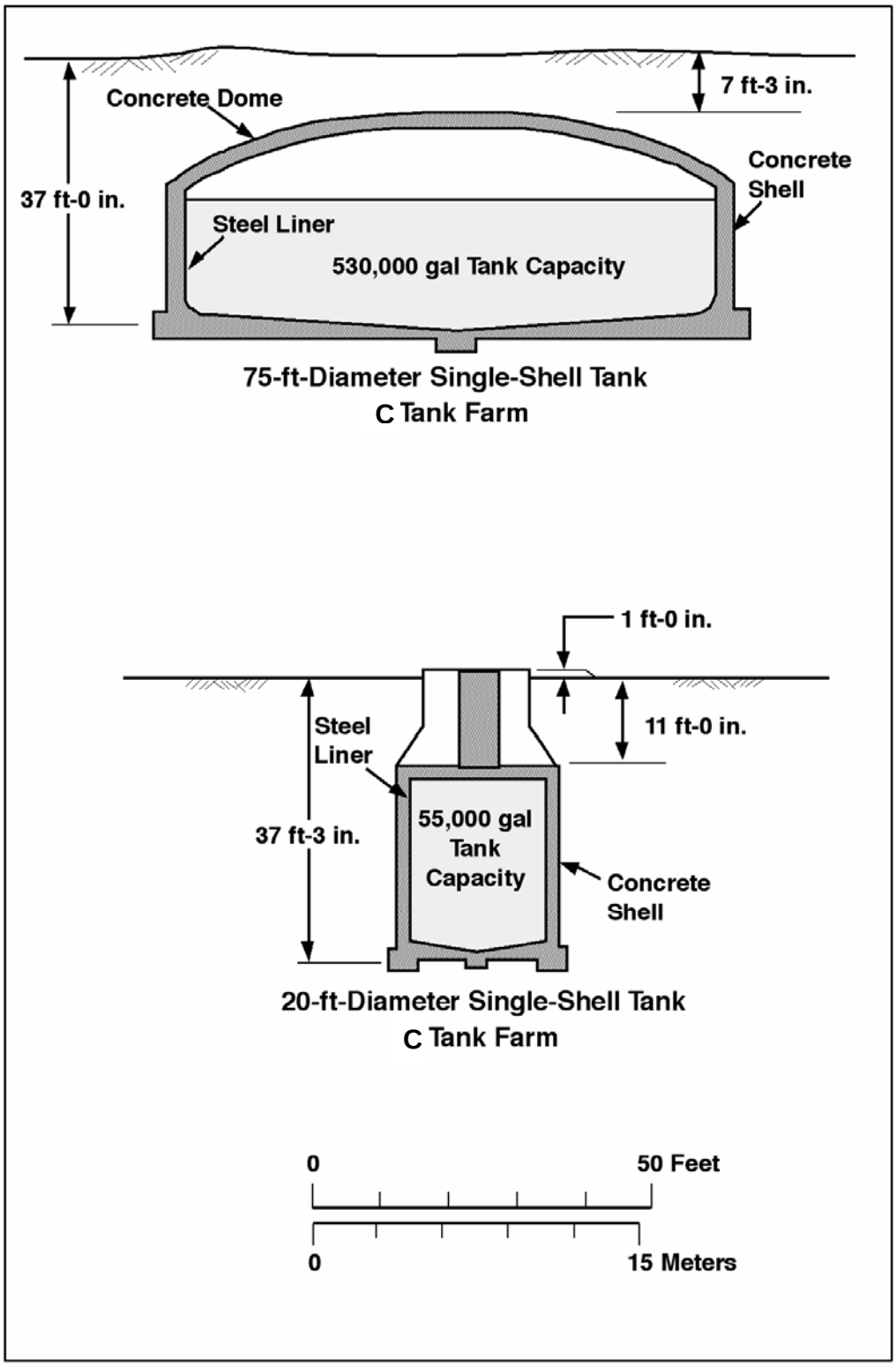

The basic tank structure consists of a carbon steel liner covered with a reinforced concrete shell that completely encases the steel liner and extends above the liner wall with a reinforced concrete dome cover over the tank. The 100-Series tanks and 200-Series tanks are situated entirely below surface with 7 and 11 feet (2 and 3.4 meters), respectively, of soil cover over the concrete tank dome. Infrastructure within the tank farm consists of buried waste transfer lines, instrument and electrical lines, abandoned water lines, and concrete structures associated with valve pits and diversion boxes. Historical data on the C tank farm including the infrastructure, waste management practices, and geologic setting are provided in RPP-14430, RPP-23748, and DOE/ORP-2005-01 (*Initial Single-Shell Tank System Performance Assessment for the Hanford Site*).

The backfill that covers the SSTs came from screened (i.e., large stones removed), excavated soil material. The heavy equipment that was used for excavation and for completing the tank construction is thought to have produced a compaction layer around each tank. The backfill between and over the tanks is relatively homogeneous compared with the undisturbed soil under the tanks.

The C tank farm 100-Series tanks were constructed in four cascades each consisting of a three-tank cascade series. Each successive tank in the cascade series is sited at a lower elevation that allowed gravity flow of liquid between tanks. Each tank is surrounded by several boreholes in which radiometric instruments were used to detect changes in activity levels in the sediments surrounding the borehole (RPP-7494, *Historical Vadose Zone Contamination from A, AX, and C Tank Farm Operations*). The C tank farm has 70 leak detection drywells drilled from 1944 to 1982. The depth ranges for most of these drywells are between 100 and 150 feet (35 and 46 meters) below ground surface. These boreholes served as both primary and secondary leak detection devices. Additionally, monitoring boreholes (i.e., groundwater monitoring wells) have been drilled in the C tank farm area.

Three of the twelve primary tanks in C tank farm (C-101, C-110 and C-111) and all four secondary tanks (C-201 through C-204) are listed in (HNF-EP-0182, *Waste Tank Summary Report for Month Ending June 30, 2006*) as confirmed or assumed leakers. HNF-EP-0182 estimates that the leak volume from Tank C-101 is 20,000 gallons (76,000 liters). As noted in RPP-14430, the tank C-101 leak estimates were based on measured liquid level drops that are equivocal because of high temperature, in-tank conditions, and unquantified evaporative loss effects. Additionally, the estimated volume of PUREX high-level supernatant that leaked does not correspond to the spectral gamma logging data from drywells around tank C-101. The estimated leak volume provided in RPP-23405, *Tank Farm Vadose Zone Contamination: Volumes Estimates for Risk Assessments*, from C-101 is 1,000 gallons (3,800 liters).

Both HNF-EP-0182 and RPP-23405 estimate the leak volume from Tank C-110 at 2,000 gallons (7,600 liter). Evidence is provided in RPP-14430 that the liquid level decrease can be attributed to measurement errors and recommended that the classification of this tank as a confirmed or assumed leak be revisited. The spectral gamma logging data and historical waste transfer records provide no evidence of leaks from this tank. HNF-EP-0182 estimates the leak volume from Tank C-111 at 5,500 gallons (20,800 liter).

HNF-EP-0182 estimates the leak volumes from the C-200-series tanks at a range of 350 to 550 gallons (1,300 to 2,100 liter). Although tanks C-111 and the C-200-series tanks are listed as "known or assumed leakers" in HNF-EP-0182, there are no spectral gamma data or documented historical record data that clearly support this classification (RPP-14430).

Waste retrieval activities are ongoing in the C tank farm and the waste volumes and associated inventories change as waste is retrieved and transferred to the double-shell tanks. As of December 2006, waste retrieval actions have been completed for tanks C-106, C-103, and the C-200-series tanks. Waste retrieval actions at tank C-108 were initiated in December 2006.

Spectral gamma data strongly indicate that tank C-105 may have leaked as indicated by contamination observed at drywell 30-05-07. RPP-23405 provides an estimated leak volume of 1,000 gallons (3,800 liters) for C-105. Concerns about the integrity of tank C-105 are supported by the historical record of large liquid level drops (approximately 3 feet (1 meter)) in tank C-105 between 1963 and 1967 (GJO-97-1-TARA, *Hanford Tank Farms Vadose Zone: Addendum to the U Tank Farm Report*). However, during that time tank C-105 stored aged PUREX high-level waste supernatant and liquid losses to evaporation are noted in the historical records (*Hanford Tank Chemical and Radionuclide Inventories: HDW Model, Rev. 4* [Agnew 1997]). The contamination in the region between tanks C-104 and C-105 has also been of interest (*Assessment of Unsaturated Zone Radionuclide Contamination Around Single-Shell Tanks 241-C-105 and 241-C-106* [Brodeur 1993], *Analysis of the 241-C Farm* [Agnew 1993]). Both cascade line and spare inlet port waste loss events have been suggested as plausible sources of contamination in this region and have been suggested as the source of contamination at drywell 30-05-07. Clear indications of waste loss from the cascade line are provided by spectral gamma data.

In contrast to other single-shell tank farms, there is only one liquid waste disposal site near the C tank farm. The 216-C-8 French drain, located about 75 feet (23 meters) southeast of the 241-C tank farm is the only liquid waste disposal facility near the C tank farm. The drain is a 6-foot (1.8-meter) diameter, 8-foot (2.4-meter) long, gravel-filled concrete pipe placed vertically below ground. It was used between June 1962 and June 1965 and received an unknown amount of ion-exchange regeneration waste from the 271-CR control house (DOE/RL-89-28, *PUREX 216-B-3 Pond System Closure/Post Closure Plan*). The waste volume was not large compared to crib discharges. There is no indication that intentional releases had any significant impact on vadose zone contamination (RPP-14430).

The CH2M HILL Hanford Group, Inc. Tank Farm Vadose Zone Project has the responsibility for all projects associated with vadose zone characterization at the tank farms under the direction of the DOE Office of River Protection. Pacific Northwest National Laboratory is currently responsible for all groundwater monitoring at the tank farms and is integrated with the Tank Farm Vadose Zone Project through the Hanford Groundwater Remediation Project, under the direction of the DOE Richland Operations Office.

2.1 TANK CONTENTS

The C tank farm received waste generated by essentially all of the major chemical processing operations that occurred at the Hanford Site, including bismuth phosphate fuel processing, uranium recovery, PUREX fuel processing, fission product recovery and tank farm interim stabilization and isolation activities. Only C tank farm was operational during the bismuth phosphate and uranium recovery processes (RPP-14430).

The C tank farm was constructed between 1943 and 1944 and first received metal waste and first cycle waste from B plant beginning in 1946. Ultimately, tanks C-101 through C-106 received metal waste and tanks C-107 through C-112 received first cycle waste. All tanks were filled with bismuth phosphate waste by the end of 1948. The 200 series tanks also received metal waste. To free up tank space, in 1952 first cycle waste was transferred to the 242-B evaporator.

Metal waste was also removed from C tank farm beginning in 1952 and transferred to U plant for uranium recovery. Ancillary equipment involved in the metal waste transfer included the 244-CR vault and diversion boxes 241-CR-151, -152 and –153. Subsequently, tributyl phosphate waste, a byproduct of the uranium recovery process, was returned to C tank farm. The 244-CR vault was modified in 1955 to scavenge tributyl phosphate waste (that is, to separate cesium-137 from the supernate by precipitation) that was present in tanks C-107 through C-112. The scavenged slurry was redeposited in tanks C-109 and C-112 to settle and the resultant supernate was discharged to the BC cribs, located about 2 miles (3.2 kilometers) south. The C tank farm and associated ancillary facilities are shown in Figure 3.

The tanks in the C tank farm currently contain an estimated total volume of 1.5 million gallons (5.68×10^6 liters) of mixed wastes consisting of various bismuth phosphate, reduction-oxidation, and PUREX processing waste streams (HNF-EP-0182). General tank content (i.e., liquid and solid volumes) data and some tank monitoring data are summarized monthly in waste tank summary reports (e.g., HNF-EP-0182).

Figure 3. Location of C Tank Farm and Surrounding Facilities.

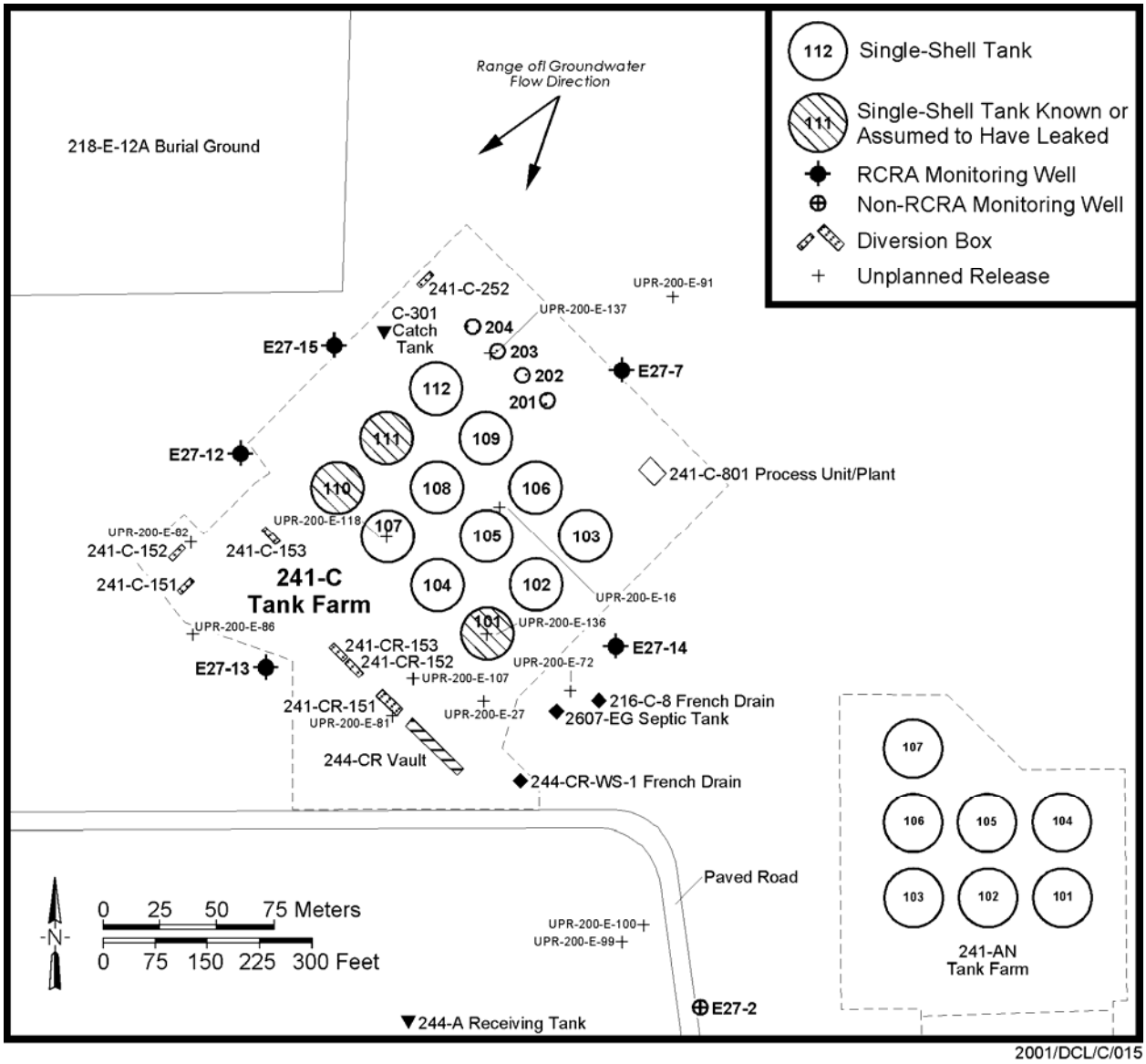

Source: RPP-16608, 2004, *Site-Specific Single-Shell Tank Phase 1 RCRA Facility Investigation/Corrective Measures Study Work Plan Addendum for Waste Management Areas C, A-X, and U*, Rev. 1, prepared by J.D. Crumpler, Columbia Energy & Environmental Services, Inc., for CH2M HILL Hanford Group, Inc., Richland, Washington.

2.2 FLUID DISCHARGE AT OR NEAR C TANK FARM

A total of 12 unplanned releases have been reported in and around the C tank farm. The unplanned releases are described in DOE/ORP-2003-11 *(Preliminary Performance Assessment for Waste Management Area C at the Hanford Site, Washington)*. The largest unplanned releases were associated with transfer of PUREX waste around 1970 and occurred near diversion boxes 241-CR-151, 241-C-151 and 241-C-152 (UPR-200-E-81, UPR-200-E-82 and UPR-200-E-86, respectively). Estimated losses ranged from 2,600 to 36,000 gallons (9,800 to 136,000 liters).

The remaining nine unplanned releases were primarily small surface spills and airborne contamination. With the exception of one above ground transfer line leak that occurred between tanks C-105 and C-108, the unplanned releases occurred outside the C farm tanks (RPP-14430).

Although the radiological inventory associated with UPR-200-E-81 near the 241-CR-151 diversion box was a reasonably low activity waste stream, it contained approximately 17,000 pounds (7,700 kg) of NO_3/NO_2 combined (RPP-15317, *241-C Waste Management Area Inventory Data Package*).

An overall assessment of the spectral gamma logging data from C farm drywells suggests that most vadose zone contamination in the tank farm originated from surface or near surface sources. This is demonstrated by relatively high concentrations of cesium-137 near surface and a general decrease in cesium-137 activity with depth. Cobalt-60 is found near the bottom of many of the drywells that manifest below near- surface cesium-137 contamination. This indicates that "mobile" cobalt-60 was driven down from subsequent recharge water (rain and snow melt). These contamination events were not generally associated with recorded events and are not comparatively significant sources of vadose zone contamination.

Figure 4, showing the major planned and unplanned release volumes of liquid waste to the soil, was generated from data presented in Sections 2.0 and 2.2, and from RPP-26744, *Hanford Soil Inventory Model, Rev. 1*. It is likely that since the releases, the mobile contaminants have migrated away from the source due to normal precipitation as well as a number of higher than normal precipitation periods and rapid snowmelt events while other contaminants, like cesium-137, have not moved as far. These recharge events would have an effect on the distribution of contaminants and moisture in the vadose zone.

The C tank farm is currently in RCRA groundwater assessment monitoring. Contaminants present in the groundwater along with potential contamination sources are discussed in PNNL-15670, *Hanford Site Groundwater Monitoring for Fiscal Year 2005*. Figure 5 shows the distribution of nitrate from recent (2005) groundwater data (PNNL-15670). The nitrate concentrations in the vicinity of C tank farm are considerably lower than that of previous SGE tank farm sites (S farm, U farm, and B complex).

3.0 DATA COLLECTION

3.1 SURVEY AREA AND COVERAGE

Remote reference electrodes were installed on August 16, 2006, as the first step in the process of resistivity data collection at the C tank farm complex. The remote reference electrodes were used for the four high-resolution resistivity (HRR) survey lines, located parallel to the fence surrounding the tank farm. The HRR lines were offset from the C tank farm perimeter fence at distances of 5 to 131 feet (1.5 to 40 meters) as necessary to avoid surface obstacles (Figure 6). The surface lines near the tank farm fence line were deployed in an effort to target near-surface characterization activities.

Figure 4. Estimated Near Surface Fluid Discharges Summary (gallons) in C Waste Management Area.

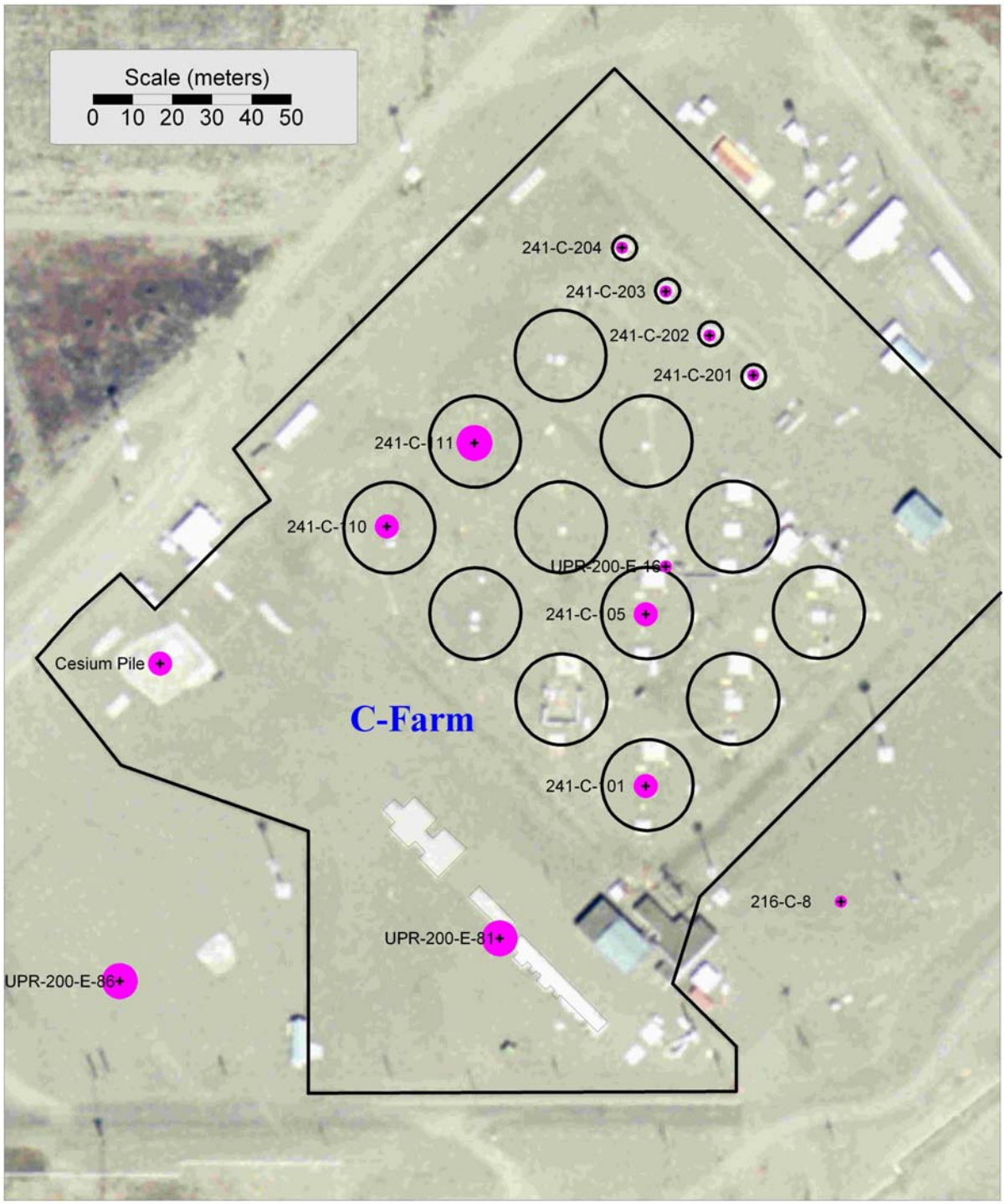

Note: Colored dots used to illustrate location and relative volume of discharges. The sizes are proportional to discharge volume. See text for discussion of specific volumes.

Figure 5. Groundwater Nitrate Concentrations (milligrams/liter) around C Tank Farm.*

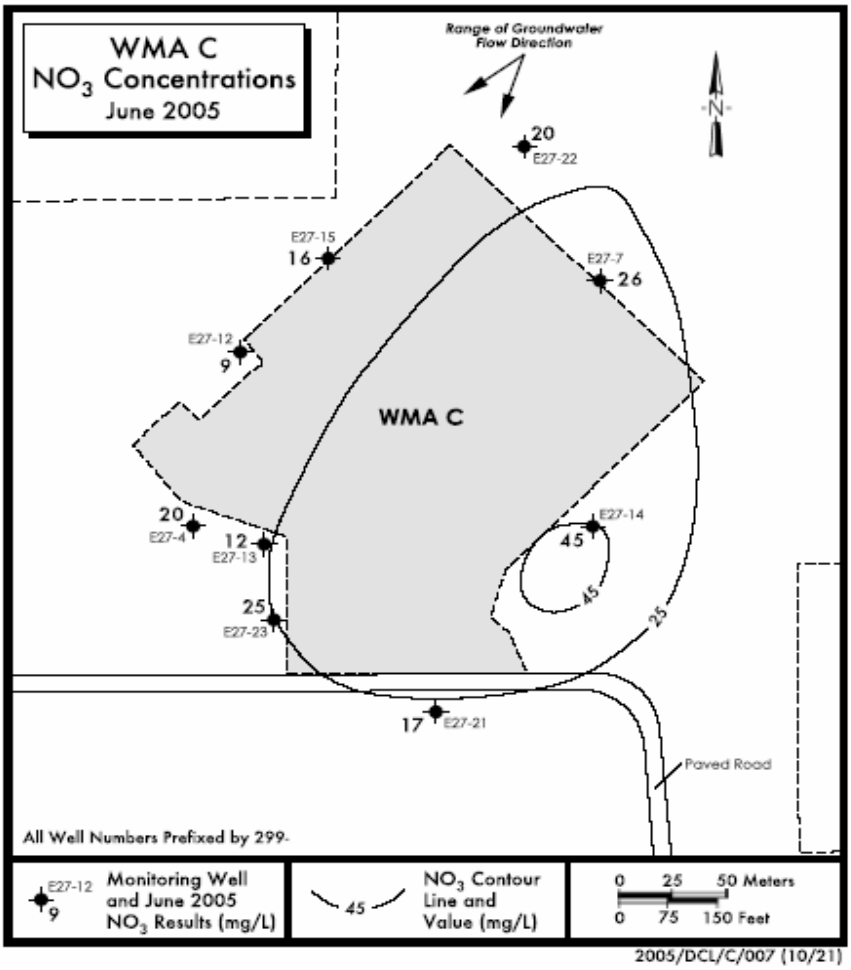

Figure 2.10-25. Nitrate Concentrations at Waste Management C Mapped for Data from the June 2005 Sampling Event

* Source: PNNL-15670, *Hanford Site Groundwater Monitoring Report for Fiscal Year 2005*, Pacific Northwest National Laboratory, Richland, Washington.

Figure 6. Geophysical Data Collection Area Showing Location of High-Resolution Resistivity Survey Lines and Wells at C Tank Farm.

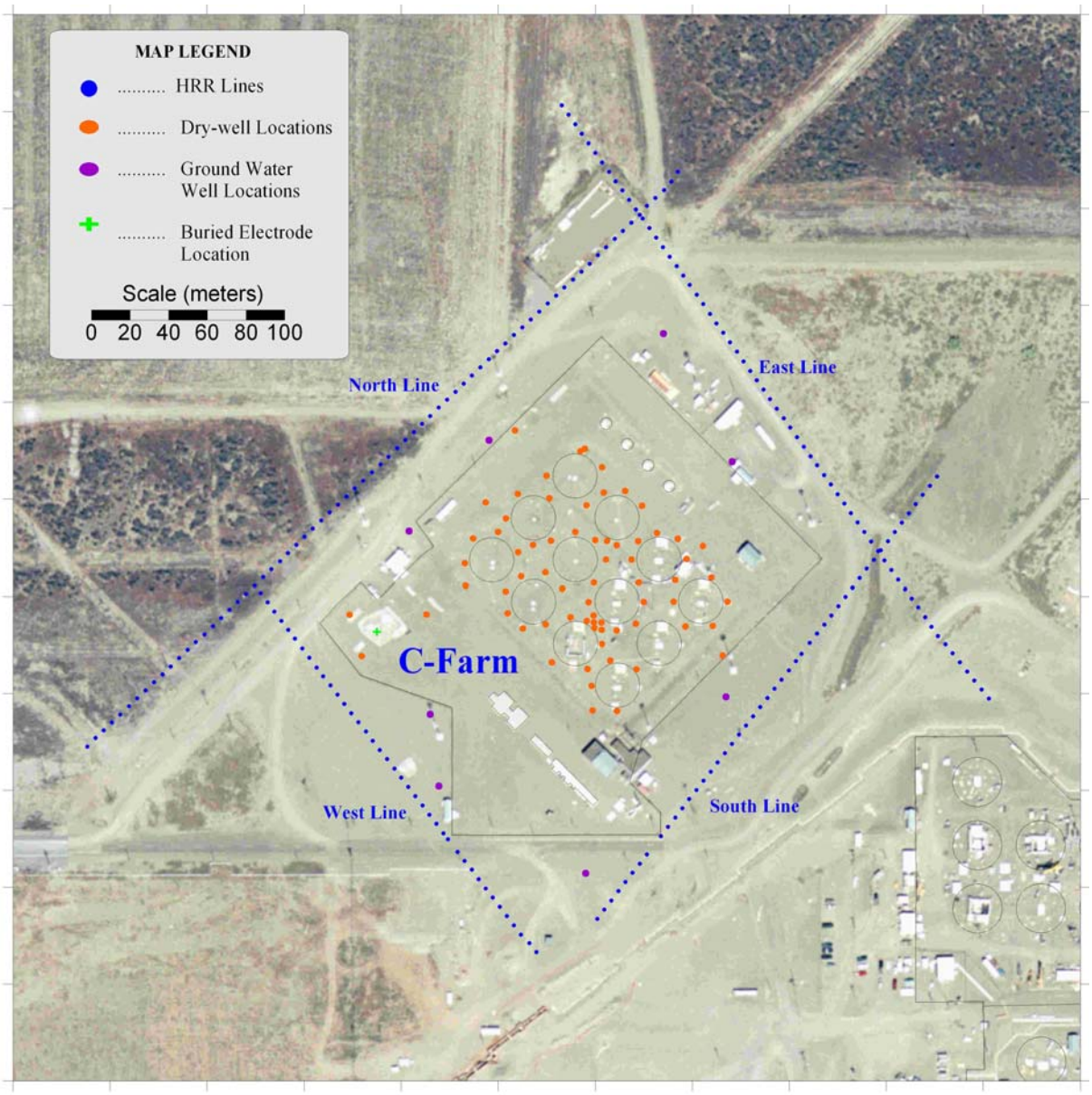

A total of 69 drywells and one buried electrode within the tank farm were used as electrode transmitters and receivers. Additionally, eight groundwater monitoring boreholes outside C tank farm were used as electrode transmitters and receivers. A summary of the data collection phases, methods, and survey coverage area can be viewed in Table 1. Table 2 lists the specific wells used in this effort and Figure 7 shows the location of the wells used for the SGE survey.

3.1.1 Surface-to-Surface Data Acquisition

Electrodes embedded into the earth's surface no more than 11 inches (28 centimeters) in a linear geometrical arrangement constitute a surface electrode array. Each of the electrode stations has the capacity to transmit current or measure voltage. Stainless steel electrode stakes were permanently installed at 20-foot (6-meter) intervals along each array. Approximately one liter of water or a weak salt solution was introduced to each electrode to reduce ground contact resistance and improve data quality. Table 1 shows that a total of 1.32 line-kilometers of surface resistivity data were collected during the STS acquisition phase between August 24 through August 26, 2006.

Table 1. Summary of Data Coverage.

Survey Phase	Date	Surface HRR			Well & Depth Electrode Tomography		
		Total Coverage	Electrode Spacing	No. Data Points	No. Wells	Well Spacing	Total No. Data Points
STS	East line 8/26/2006	378 m	6 m	1,952	N/A	N/A	N/A
	West line 8/26/2006	234 m	6 m	737			
	North line 8/25/2006	426 m	6 m	2,473			
	South line 8/24/2006	282 m	6 m	1,106			
WTS	East line 8/26/2006	NA	6 m	4,723	77 wells 1 depth electrode	5 – 300 m	17,584
	West line 8/26/2006		6 m	2,917			
	North line 8/25/2006		6 m	5,282			
	South line 8/24/2006		6 m	4,662			
WTW	Forward 8/25/2006	NA	NA	2,799	77 wells 1 depth electrode	5 – 300 m	5,698
	Reverse 8/25/2006			2,899			

HRR = high-resolution resistivity.
m = meter.
NA = not applicable.
STS = surface-to-surface.
WTS = well-to-surface.
WTW = well-to-well.

Table 2. Wells Used for Surface Geophysical Exploration Survey.

Well ID	SuperSting R8* Channel	Well ID	SuperSting R8* Channel	Well ID	SuperSting R8* Channel
30-00-01	1	30-05-02	27	30-09-02	53
30-00-03	2	30-05-03	28	30-09-06	54
30-00-06	3	30-05-04	29	30-09-07	55
30-00-09	4	30-05-05	30	30-09-10	56
30-00-10	5	30-05-06	31	30-09-11	57
30-00-11	6	30-05-07	32	30-10-01	58
30-05-10	7	30-05-08	33	30-10-02	59
30-00-13	8	30-05-09	34	30-10-09	60
30-00-22	9	Buried Electrode	35	30-10-11	61
30-00-24	10	30-06-02	36	30-11-01	62
30-01-01	11	30-06-03	37	30-11-05	63
30-01-06	12	30-06-04	38	30-11-06	64
30-01-09	13	30-06-09	39	30-11-09	65
30-01-12	14	30-06-10	40	30-11-11	66
30-03-01	15	30-06-12	41	30-12-01	67
30-03-03	16	30-07-01	42	30-12-03	68
30-03-05	17	30-07-02	43	30-12-09	69
30-03-07	18	30-07-05	44	30-12-13	70
30-03-09	19	30-07-07	45	299-E27-15	71
30-04-01	20	30-07-08	46	299-E27-12	72
30-04-02	21	30-07-10	47	299-E27-13	73
30-04-03	22	30-07-11	48	299-E27-23	74
30-04-04	23	30-08-02	49	299-E27-21	75
30-04-05	24	30-08-03	50	299-E27-14	76
30-04-08	25	30-08-12	51	299-E27-7	77
30-04-12	26	30-09-01	52	299-E27-22	78

*SuperSting R8 is a trademark of Advanced Geosciences, Inc.

Figure 7. Location of Drywells and Monitoring Boreholes Used for Surface Geophysical Exploration Survey.

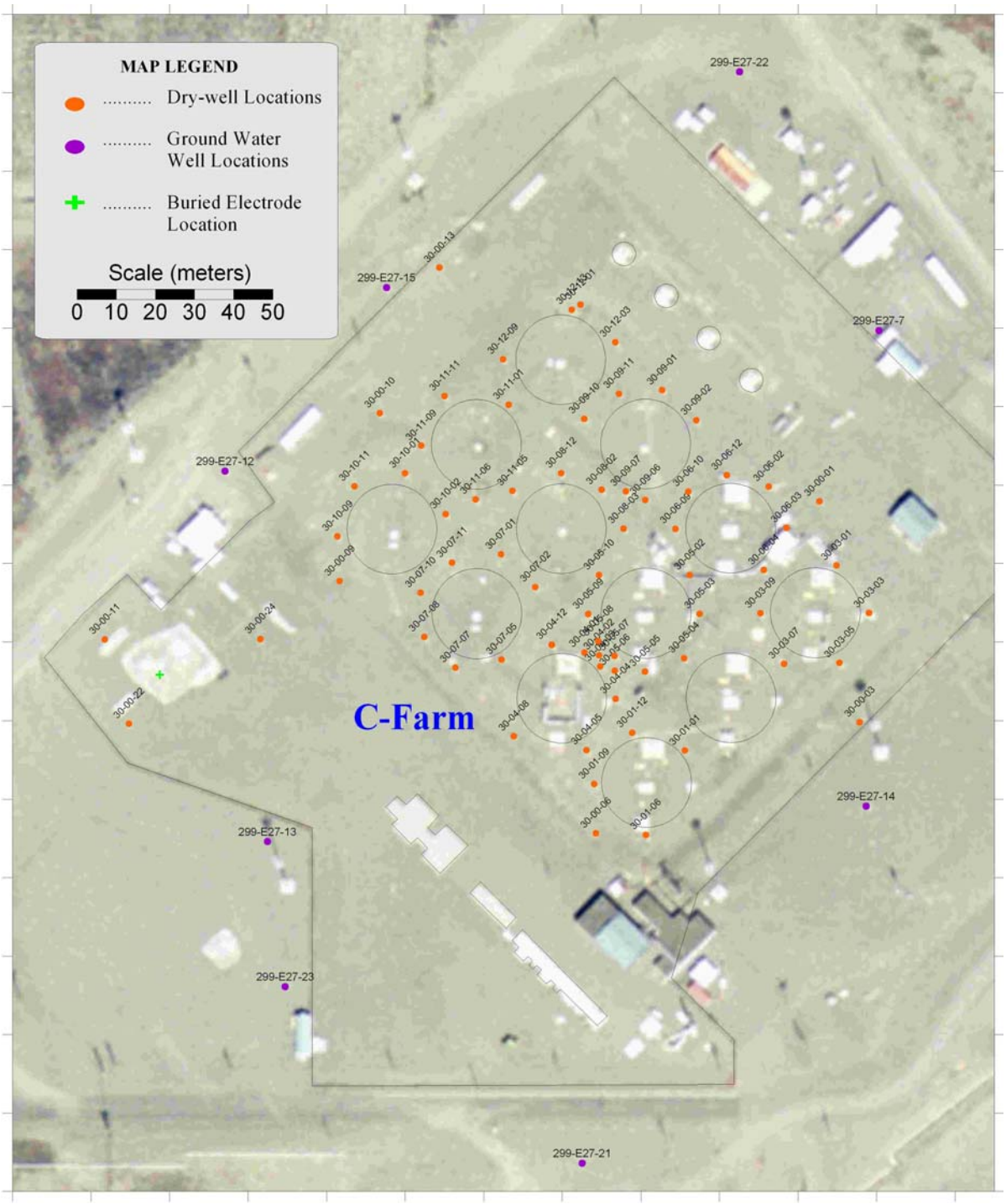

3.1.2 Well-to-Surface and Buried Electrode-to-Surface Data Acquisition

WTS and buried electrode-to-surface data acquisition follows the same logic presented in the section above; however, the geometry with respect to drywells, monitoring boreholes, buried electrodes, and surface electrodes is distinct from a linear surface array. With WTS and buried electrode-to-surface data acquisition, the wells and buried electrode(s) act as the source current, while the surface stations are reserved as receiving electrodes for recording of voltage measurements.

3.1.3 Well-to-Well and Well-to-Buried Electrode Data Acquisition

WTW and well-to-buried electrode (WTBE) data acquisition follows the same process presented in the above sections. The major difference is the geometry of the electrodes with respect to the wells. The typical electrode used in electrical resistivity is a surface electrode, which is imbedded no more than 11 inches (28 centimeters) into the ground by design. For all practical purposes, the surface electrode can be represented as a point in model space. A drywell monitoring borehole, however, is a very long electrode that must be modeled as a line source in the model. Furthermore, wells are not generally distributed in a linear fashion. Thus, the end result is a more complex geometrical configuration of sources and receivers which are used to generate a record of observed measured voltage potentials in a fixed sequence of time.

For the WTBE, a single electrode was installed at a depth of 59 feet (18 meters) below the ground surface in order to help provide depth information in the WTW inversions. For completeness, reciprocal measurements of WTBE and buried electrode-to-well measurements were acquired.

The HRR survey uses a four-electrode array where electric current is injected into the earth through one pair of electrodes (transmitting pole) and the resultant voltage potential is measured by the other pair of electrodes (receiving pole). Reciprocal measurements are recorded where each electrode is used as a receiving and transmitting electrode. In this way, two data sets are generated (forward and reverse) under each geometric array configuration. Figure 8a and Figure 8b show the forward and reverse measurements for the pole-pole configuration, where for each electrode pair one of the electrodes (electrodes 3 and 4) are effectively at infinity. Electrical theory shows that reciprocal measurements should be nearly equal when acquired under heterogeneous earth conditions. Therefore, comparison of the reciprocal measurements is an effective tool for detecting suspect data, or data influenced by subsurface infrastructure.

Figure 8a. Forward Pole-Pole Electrode Measurement.

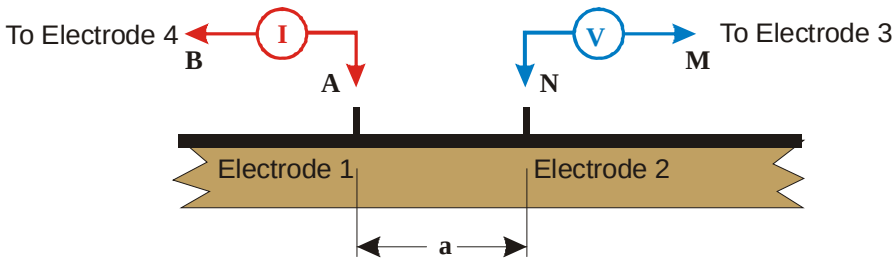

Figure 8b. Reverse Pole-Pole Electrode Measurement.

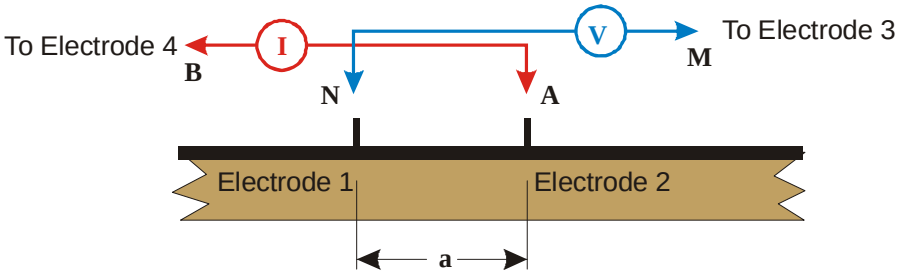

Where:

I	=	Current electrode pair
V	=	Voltage electrode pair
B	=	Remote Reference Current Electrode (placed at infinity)
M	=	Remote Reference Voltage Electrode (placed at infinity)
N	=	Local voltage electrode
A	=	Local current electrode
a	=	distance between electrodes

3.2 INSTALLATION AND SETUP

Following the installation of the remote reference electrode arrays, individual 16-gauge wires were strung from a central location outside the C tank farm fence to each of the 77 wells and one depth electrode that would be used as sources and receivers. Wells were prepared in one of two ways: (1) by removing a small area of rust from the well casing and sandwiching a short length of wire between the well casing and the expansion plug used to seal the drywell, or (2) using hose clamps to attach the wire to monitoring components inside the well casing. The wires from the wells were then connected to an hydroGEOPHYSICS, Inc. patch panel which organizes the 77 wells and one depth electrode wires and acted as a coupler to the SuperSting R8[4] switch boxes. By distributing the measurements in a logically structured method, the switch boxes act as a multiplexer to the SuperSting R8 keeping the data structured. Figure 9 is a photo showing the equipment setup and Figure 10 shows the wire-to-well connection.

[4] SuperSting R8 is a trademark of Advanced Geosciences, Inc.

Figure 9. Equipment and Setup for the Well-to-Surface Survey.

Figure 10. Field Worker Attaching Wire to Well.

3.2.1 Installation of Remote Reference Arrays

Remote reference electrode arrays were established approximately 1 mile (1.7 kilometers) from the survey to the northwest and the northeast of the tank farm site. Each array consisted of 11 stainless steel rods that were driven into the ground and connected together with 10 gauge insulated copper ground wire. A weak salt solution was introduced to each electrode in the source array while water was introduced to each electrode in the receiving array to reduce ground contact resistance and improve data quality. Both remote arrays were connected to the SuperSting R8 using 16 gauge wire. The wire was strung along access roads and through open fields avoiding site infrastructure. The connection of the resistivity equipment to the remote reference electrodes completed the HRR four pole measurement system. A more detailed description of the installation practice can be viewed in RPP-RPT-28955, *Surface Geophysical Exploration of T Tank Farm*.

3.2.2 Permanent Surface Electrodes

Permanent surface electrodes were installed along four survey lines to streamline the data acquisition activities and improve future data acquisition repeatability. Each electrode consisted of 1/2-inch (1.3 centimeters) diameter stainless-steel rod in the shape of a "T." The top horizontal bar rested on the ground surface, increasing electrode to ground contact and limiting the electrode penetration to 11 inches (28 centimeters). Additionally, the top bar also provided a suitable location for connecting the data acquisition cable. The installation of permanent electrodes provides cost reduction as they can be installed without impacting data acquisition time, and once installed can be used many times.

3.2.3 Resistivity Equipment

Electrical measurements were acquired using a SuperSting R8 in a pole-pole array configuration. A combination of passive cables using automated electrode switching boxes, and active cables where the electrode switching is performed on the cable, were used to connect the surface electrodes to the SuperSting R8 data acquisition unit. Two 12-volt direct current marine deep cycle batteries were used to supply input power. The batteries and power cable were strictly controlled using appropriate lockout and tagout procedures. A more comprehensive description of the equipment can be viewed in RPP-RPT-28955.

3.2.4 Weather Conditions

The survey weather conditions included clear days with temperatures ranging from 75 to 90 degrees Fahrenheit. Figure 11 is a photo showing the environmental conditions under which the survey was completed.

Figure 11. Environmental Conditions During the Survey.

4.0 ANALYSIS RESULTS AND INTERPRETATION

The methodology used for the C tank farm investigation parallels the recently completed SGE investigation of the U tank farm (*Surface Geophysical Exploration of U Tank Farm at the Hanford Site* [RPP-RPT-31557]). A description of the data processing methods, theory, and limitations associated with using electrical resistivity methods in a tank farm environment are described in RPP-RPT-28955.

A combination of the size of the tank farm, data collection design, and quality of the surface data provided mixed results from the initial resistivity investigation at the C tank farm. The physical size of the tank farm coupled with the location of the surface lines used for data collection produced more data than could be modeled at one time, given the current computer software and hardware limitations. To perform the resistivity analysis, the model domain had to be broken up into smaller subsets. As a result of the site complexity and modeling limitations, more than 12 different data combinations and model parameters were modeled, which was more than twice that of U farm. Data confidence is greatest where several inversion models are completed using different electrode data sets and/or inversion constraints while still producing similar results. However, despite the increased modeling effort, the individual data subsets produced varying results with a low degree of repeatability. The varying results seem to be caused by the inability to honor the complete data set under this investigation. The well-to-well with the drywell-only data produced the best results in terms of modeling statistics and data confidence. Different aspects of the analysis are discussed in the following sections.

4.1 SURFACE-TO-SURFACE ELECTRICAL RESISTIVITY INVERSION

Resistivity data were collected using a set of four orthogonal STS lines around the perimeter of the C tank farm using the pole-pole resistivity array. Logistical considerations, such as multiple road crossings, limited data acquisition to a two-dimensional field setup where each surface line was collected separately. The STS collection effort included lines labeled "North Line," "East Line," "West Line," and "South Line." The two-dimensional processing and results were used to support the three-dimensional processing by providing a quality control inversion step. The inversions of the two-dimensional profiles were not very successful. However, the lack of success of two-dimensional inversion does not necessarily indicate a failure of the data to present a coherent result in three-dimensions. The S tank farm results (RPP-RPT-30976, *Surface Geophysical Exploration of S Tank Farm at the Hanford Site*) is a good example where two-dimensional inversion results were not as successful as the three dimensional inversion.

Results of the two-dimensional processing can be viewed in Appendix A as Figures A-1 through A-6. Each plot shows the STS data in the standard HRR data format and plotted as apparent resistivity and inversion results using the software EarthImager2D[5]. The common HRR plotting methodology is presented in RPP-RPT-28955.

Data quality for the east and west lines was acceptable and a small percentage of points were removed as part of the filtering and spike rejection process. Table 3 shows the number of data points collected along each line, the number of data points rejected, the percentage of points kept and the inversion fitting parameters for the two-dimensional fitting parameters. The S tank farm report (RPP-RPT-30976) discusses the data rejection procedure. Both east and west lines rejected less than 10% of the data.

Table 3. Resistivity Data Statistics for the HRR and EarthImager2D* Inversion Procedures.

Data Parameters	East Line	West Line	North Line	South Line
Raw data points	1952	737	2473	1106
Rejected data points	136	70	461	166
% retained	93.0	90.5	81.3	84.9
Root mean square error	2.92	5.24	6.35	2.97
L2 Normalization	0.94	3.04	4.47	0.98

* EarthImager2D is a trademark of Advanced Geosciences, Inc.

The primary objective of inversion is to reduce data misfit between field measurements of transfer resistance (voltage/current) and calculated data for a reconstructed resistivity model. This misfit is typically equivalent to the measurement error, which usually ranges from 1% to 5%. Reducing the misfit to less than the measurement error may cause the model to overfit the data and replicate noise. A misfit larger than the measurement error indicates that the reconstructed model is not representative of subsurface electrical properties. The goodness of

[5] EarthImager2D is a trademark of Advanced Geosciences, Inc.

the misfit may be characterized by the root mean square (RMS) error or the L2 Normalization. The RMS is defined as:

$$RMS = \sqrt{\frac{\sum_1^N \left(\frac{d_i^{Pred} - d_i^{Meas}}{d_i^{Pred}} \right)^2}{N}} \cdot 100 \qquad (4\text{-}1)$$

Where:

N	=	the total number of measurements
d^{Pred}	=	the predicted data
d^{Meas}	=	the measured data.

The RMS statistic is more heavily weighted toward those points with a larger fitting error. Additionally, the RMS error is an average data misfit over all data points. A single erroneous data point could lead to a large RMS error. For example, consider a data set of 100 measurements (N=100). As an extreme case, the measured voltage is 1mV; however, the predicted voltage is 1V. If there is a perfect fit (no errors) to all other 99 data points, the RMS error would be 9.99% due to this single erroneous data point. To overcome this large RMS fitting error problem, the bad point can be removed from the dataset and the inversion rerun.

L2 Normalization is another measure of data misfit and is defined as the sum of the squared weighted data errors:

$$L2Norm = \frac{\sqrt{\sum_1^N \left(\frac{d_i^{Pred} - d_i^{Meas}}{W_i} \right)^2}}{N} \qquad (4\text{-}2)$$

Where:

N	=	the number of measurements
W_i	=	the data weight as calculated from the covariance from the data error
d^{Pred}	=	the predicted data
d^{meas}	=	the measured data.

Both RMS and L2 describe a goodness of fit in a slightly different way. From the statistics in Table 3, the east and south lines both have good fits to the data, indicating that the inversion results are a good match to the measured data. The west and north lines have slightly worse fits, which could possibly be due to the near-surface interferences from infrastructure or dimensionality of the problem (two-dimensional modeling of a three-dimensional phenomenon).

4.2 WELL-TO-WELL ELECTRICAL RESISTIVITY INVERSION

The WTW inversion modeling was accomplished in two steps using the inversion code EarthImager3D[6]. Initial inversion results were calculated using resistivity data collected only on the steel-cased drywells. A total of 69 drywells were included as part of the initial inversion calculation. The casing lengths ranged between 15 and 47 meters with the water table located approximately 65 meters below ground surface. The drywells do not contact the water table. The drywell naming convention at C farm follows a "30-AA-BB" format, where AA is the last two digits of the local tank name and BB is the clock position of the well with respect to the north direction where north is at 12 o'clock. An additional resistivity data set was acquired and inverted using the seven groundwater monitoring boreholes in conjunction with the drywells. The groundwater monitoring boreholes are located at the perimeter of the C tank farm footprint and extend as deep as 94 meters below ground surface.

One additional electrode that was used in the C tank farm resistivity characterization was buried directly west of the tanks, beneath a pipeline leak at approximately 17 meters below ground surface. The buried electrode was placed in response to recommendations made as part of the T tank farm report (RPP-RPT-28955), where it was suggested that the vertical resolution of resistive anomalies could be better resolved if point sources are included with wells. The buried electrode was placed in borehole C5107 adjacent to C-152 Diversion Box, in a location known as "The Cesium Pile."

Figure 12 and Figure 13 shows the results of the inversion using drywells only near the footprint of the tanks. The three-dimensional WTW inversion results are shown in plan view due to the unreliability of vertical information in this type of modeling. The smaller, dark-colored resistivity plume represents values up to 4.5 ohm-meters and the larger light-colored plume represents values up to 6.5 ohm-meters.

The spatial location of the groundwater monitoring boreholes with respect to the densely concentrated drywells required a large inversion modeling domain. The computational memory requirements for a single domain that included all drywells and groundwater wells exceeded the Microsoft Windows XP[7] four gigabyte memory limit. As a result, four smaller inversion domains were selected to reduce the total number of ground water wells used for each inversion. Figure 14 shows an aerial view of the C farm project site with colored rectangles that represent the individual modeling domains that were completed. Each rectangle bounds a small subset of the total data set that was acquired. For example, the WTW north domain included data from only the 299-E27-14, 200-E27-15, 299-E27-12, and all but three of the drywells. The west and north domains include the buried electrode (C5107).

[6] EarthImager3D is a trademark of Advanced Geosciences, Inc.
[7] Microsoft and Windows XP are trademarks of the Microsoft Corporation.

Figure 12. WTW Inversion Results using Drywells Only.

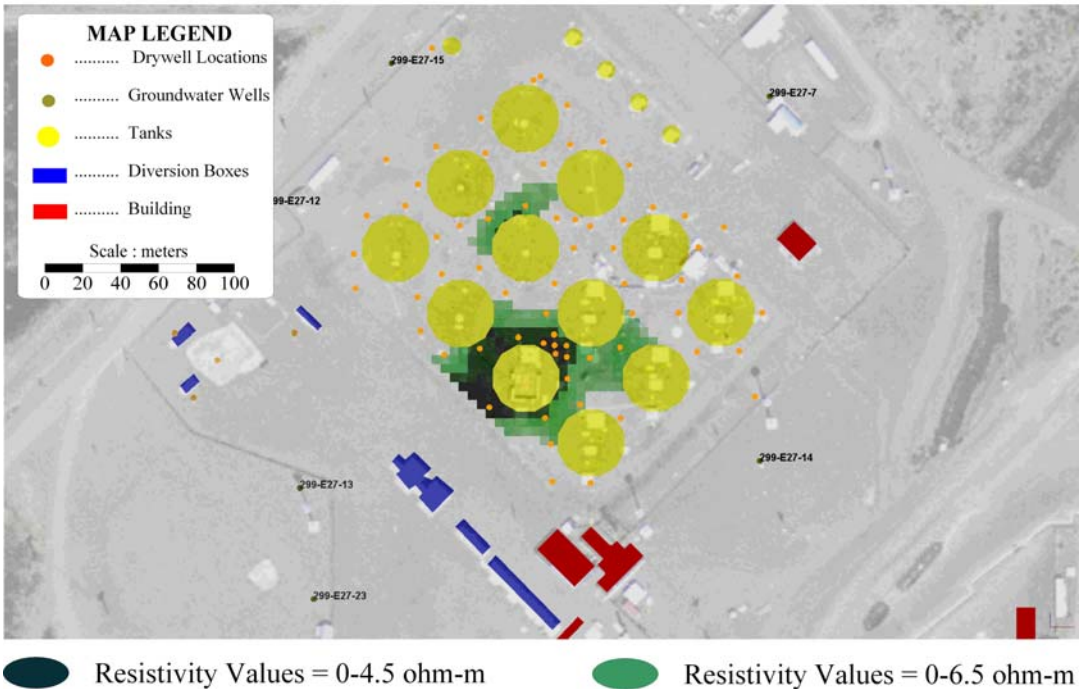

Figure 13. WTW Inversion Results using Drywell Only Data Showing Detail Around C-104.

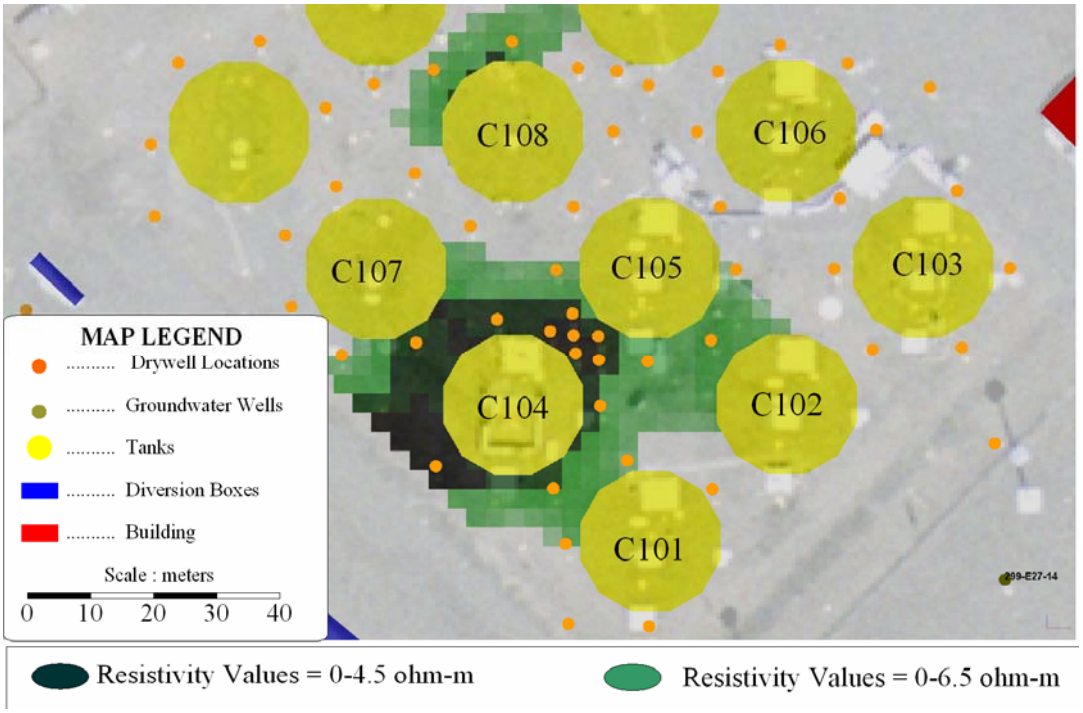

Figure 14. Map of C Farm Showing WTW Inversion Modeling Domains.

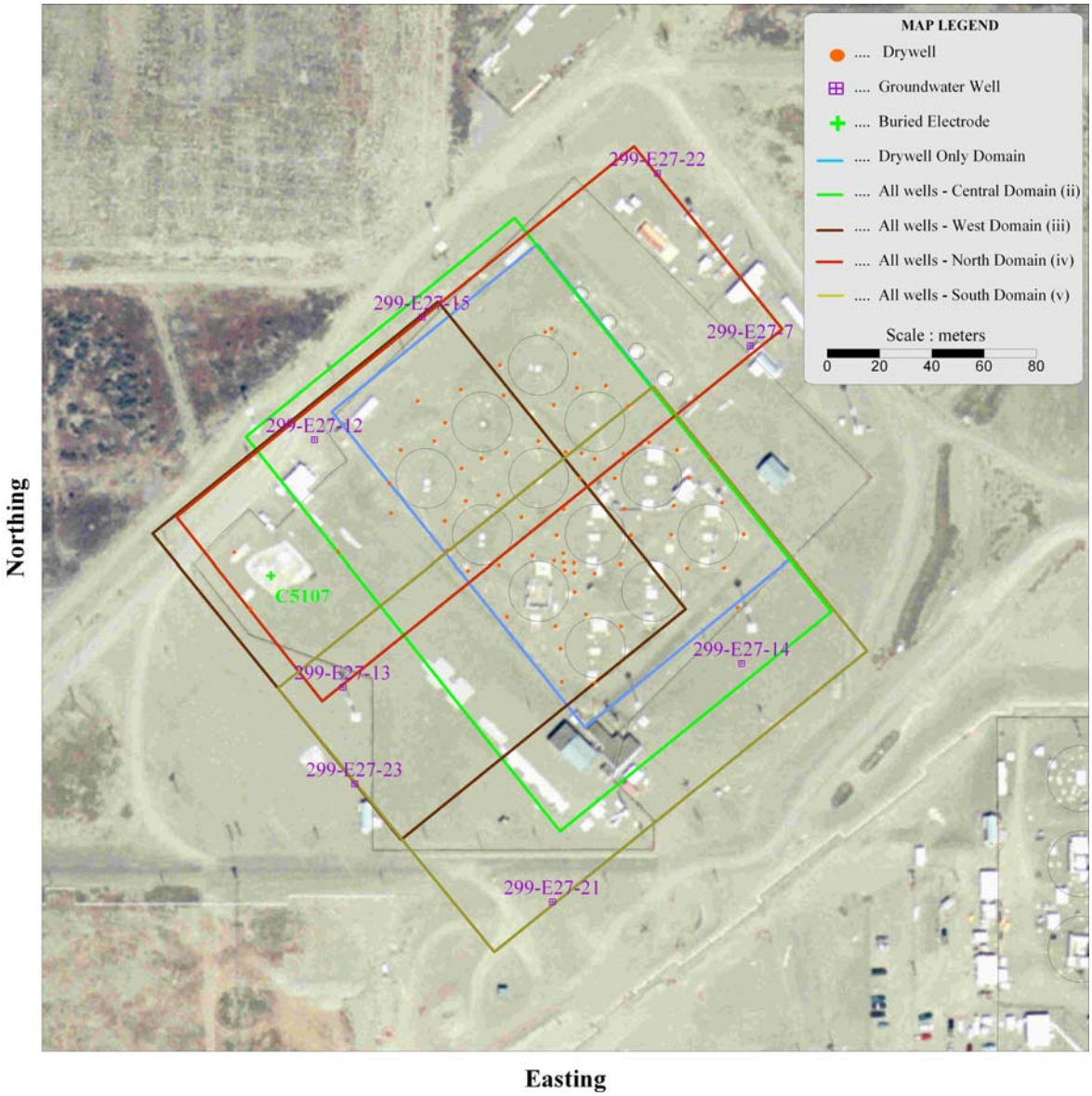

Breaking the data into separate domains reduces the memory requirements by greatly reducing the data population and model cells used to generate each model. The drawback to domain reduction is the reduced amount of measured data in the inversion modeling. If, for example, the area were broken into two domains, only one quarter of the data would be available for each domain. An effort was made to overlap the different domains where possible. Table 4 shows a comparison of the data coverage and inversion results for the five WTW modeling domains. The last column of the table describing Data Range refers to the small and large solid color isopleths used in rendering the resistivity plumes (e.g., Figure 12).

Table 4. Comparison of WTW Inversion Results for the Individual Modeling Domains.

Data Type	Model	Data Points Used	% of Data Population	Convergence			Data Range (ohm-meter)	
				Itera-tions	RMS	L2	Small	Big
WTW drywell only	Single	3,215	74	24	4.9	1.0	4.5	6.5
WTW drywell & monitoring borehole	Central	3,287	59	20	5.0	0.7	4.5	6.5
	West	1,767	32	20	8.7	2.1	N/A	N/A
	North	919	16	14	4.6	0.6	12.0	15.0
	South	1,857	33	20	8.6	2.9	N/A	N/A

L2 = L2 Normalization.
N/A = Not applicable, data set was not plotted since convergence parameters were not acceptable.
RMS = root mean squared.
WTW = well-to-well.

Two of the four WTW drywell and groundwater well domains produced RMS errors greater than 5 and L2 Normalization values greater than 1.3. Previous experience with T, S, and U farm SGE data showed that analyses exceeding these thresholds produced suspect results. Therefore, the WTW west and south domains were not plotted. The WTW central and north domains produced acceptable convergence data; however, results were inconsistent along the common boundaries with other models. The inconsistency reduced confidence in the results. The WTW central domain produced similar spatial resistivity anomalies and a similar resistivity value range to the WTW drywell only (see Figure 14). However, the WTW north domain, which overlaps the WTW central domain, produced no resistivity anomalies within the resistivity value range of Figure 12. The inconsistent result is likely due to the different perspective that each data set generates.

Splitting the data set into separate domains produced varied results and with few similarities between individual inversions even in areas of data overlap. For this reason the graphical results are not displayed within this section. However, a more detailed discussion of the inversion domain limitations is provided in section 6.2, Model Domain Limitations, and includes several graphical inversion results. The graphical results within section 6.1 are strictly for the purposes of demonstrating the effects of breaking the domain into separate subsets. The modeling effort has provided a significant data quality assessment and modeling parameters that can be used to streamline modeling if and when the entire data set is inverted within a single domain.

4.3 WELL-TO-SURFACE ELECTRICAL RESISTIVITY INVERSION

The WTS inversion modeling was performed in an attempt to gain further insight to the subsurface of the C tank farm. Previous attempts to model WTS data, at T farm (RPP-RPT-28955) and at U farm (RPP-RPT-31557), resulted in high levels of noise and contributed less to the overall interpretation of the results when compared to the WTW data. The noise observed in the WTS data acquired at T tank farm was likely due to the positioning of the surface electrodes. The surface electrodes were installed within the farm near the T tank farm infrastructure (e.g., pipes, tanks), and similar to STS inversion, were unable to produce a

coherent or consistent result. Conversely, at the C tank farm the surface electrodes were located around the exterior perimeter in the same manner as the U tank farm SGE deployment.

The spatial coverage of the area bound by the surface electrodes at C tank farm was greater than the WTW area and was 1.53 times larger than U tank farm. The increased coverage resulted in a domain that exceeded the software and hardware limitations of the current inversion software. Therefore, the data set was divided into three smaller subset domains in the same manner as described in the WTW section.

Figure 15 shows an aerial view of the C farm project site with three distinct modeling domains outlined. The west and north domains included the buried electrode (C5107). As with the WTW modeling effort, breaking the data into separate domains greatly reduced the data population and resulted in a variety of resistivity results. The WTS south and west domains produced the most similar results but were in contrast to the results of the north domain. Table 5 shows a comparison of the inversion results for the three WTS modeling domains. All three domains produced acceptable convergence parameters, despite the largest domain area containing less than 30% of the total data population.

The reliability of the surface data, whether as STS or WTS, is questionable due to the limited coverage of the four perimeter lines. The individual lines presented in Appendix A show some regions that are highly conductive, likely a result of infrastructure interference. The success of the WTS data results for C tank farm SGE is questionable due to the surface electrode locations and breaking the data sets into separate domains. It is difficult to assess, prior to data collection, whether a set of surface electrodes will experience significant interferences from infrastructure. In retrospect, the electrode geometry may have been too sparse to adequately constrain the inversion model. This is most significant on the southwest and northeast lines where the distance between the survey line and the drywells is greater than 300 feet (92 meters). However, the similarity of results for two of the three domains suggests that valuable information may be achieved if inverted as a single domain. A more detailed discussion of the inversion domain limitations is discussed within Section 6.1, Model Domain Limitations, and includes several graphical inversion results. The graphical results within Section 6.1 are strictly for the purposes of demonstrating the effects of breaking the domain into separate subsets.

Figure 15. Map of C Farm Showing WTS Inversion Modeling Domains.

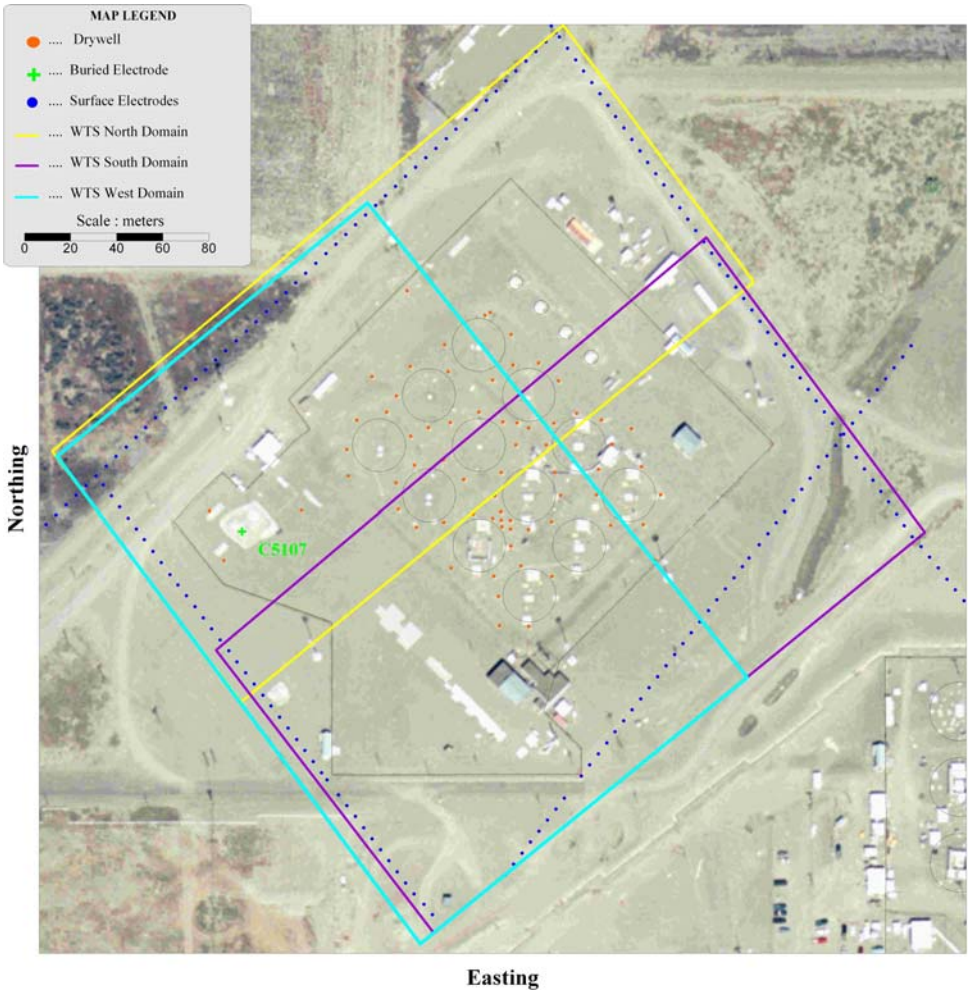

Table 5. Comparison of WTS Inversion Results for the Individual Modeling Domains.

Data Type	Model	Data Points Used	% of Data Population	Convergence			Data Range (ohm-meter)	
				Itera-tions	RMS	L2	Small	Big
Well-to-surface	South	3,688	23	10	4.9	0.7	2.0	6.5
	North	3,372	21	19	5.1	0.7	15.0	20.0
	West	4,553	28	12	5.3	1.1	5.0	6.5

L2 = L2 Normalization.
N/A = Not applicable, data set was not plotted since convergence parameters were not acceptable.
RMS = root mean squared.
WTS = well-to-surface.

4.4 COMBINATION WELL-TO-WELL, WELL-TO-SURFACE, AND SURFACE-TO-SURFACE ELECTRICAL RESISTIVITY INVERSION

The last resistivity inversion trial for C tank farm SGE is a combination data set that includes two groups, (1) WTW and STS, and (2) WTW, WTS, and STS data. Due to the large domain of the entire data set, two data subsets were chosen that reduced the domain size and made the inversion problem more tractable. Figure 16 shows an aerial view of the C farm project site with two colored rectangles that represent the individual modeling domains. The modeling domain area for the two inversion combination groups is identical.

Table 6 shows a comparison of the final inversion results for the four combination modeling domains. Initially, two of the domain areas produced RMS errors greater than five. Multiple inversion models were run for each of the domain areas in order to reduce the RMS error and improve data convergence. Results for each inversion were analyzed and electrodes associated with the high RMS were excluded and then the inversion was re-run. Although this process further reduced the data population associated with each domain area, it did improve the model convergence parameters. The largest domain area contained less than 30% of the total data population.

Of the four combination models, only the WTW and STS south domain area produced convergence results that were acceptable; RMS less than 5 or L2 Normalization less than 1.3. The WTW and STS north domain area exceeded the available memory before a suitable number of iterations could be performed that would allow better data convergence. As discussed in the previous sections, the reliability of the surface data, whether as STS or WTS, is questionable due to the limited geometry of the four perimeter lines. The combination inversion models were expected to produce suspect and variable results based on the experience with previous modeling of the WTW, WTS and STS data. However, it was hoped that the combination of the three different data parameters might provide more consistency between the north and south domain areas. The convergence parameters were not adequate enough for the results to render a reliable interpretation. However, a more detailed discussion of the inversion domain limitations is discussed within Section 6.1, Model Domain Limitations, and includes several graphical inversion results. The graphical results within Section 6.1 are strictly for the purposes of demonstrating the effects of breaking the domain into separate subsets. As a group, the models produced an average RMS of 6.3 and an L2 Normalization of 1.3, which suggests that accurate and reliable inversion results are possible when run as a single domain with all data.

Model convergence could only be improved after analysis of a completed inversion where modelers could then remove data points associated with high RMS. The reduced data set was then re-inverted. Several of the inversion results had an initially high RMS after the first trial run. These high RMS values could be as great as 8% to 9%, and were usually the result of a small subset of inconsistent voltage readings. To overcome the high RMS, the original data were filtered to remove those individual data with relative errors between measured and modeled voltages greater than 10%. This step typically removed between 15% and 25% of the original data. The inversion algorithm was rerun with the smaller subset of measured data, with the result of lowering the final RMS of the model to an acceptable level. With the combined steps of domain reduction and rerunning the inversion after removal of high RMS, the number of models increased by 4 to 8 times over the U farm modeling effort.

Figure 16. Map of C Farm Showing Combination Inversion Modeling Domains.

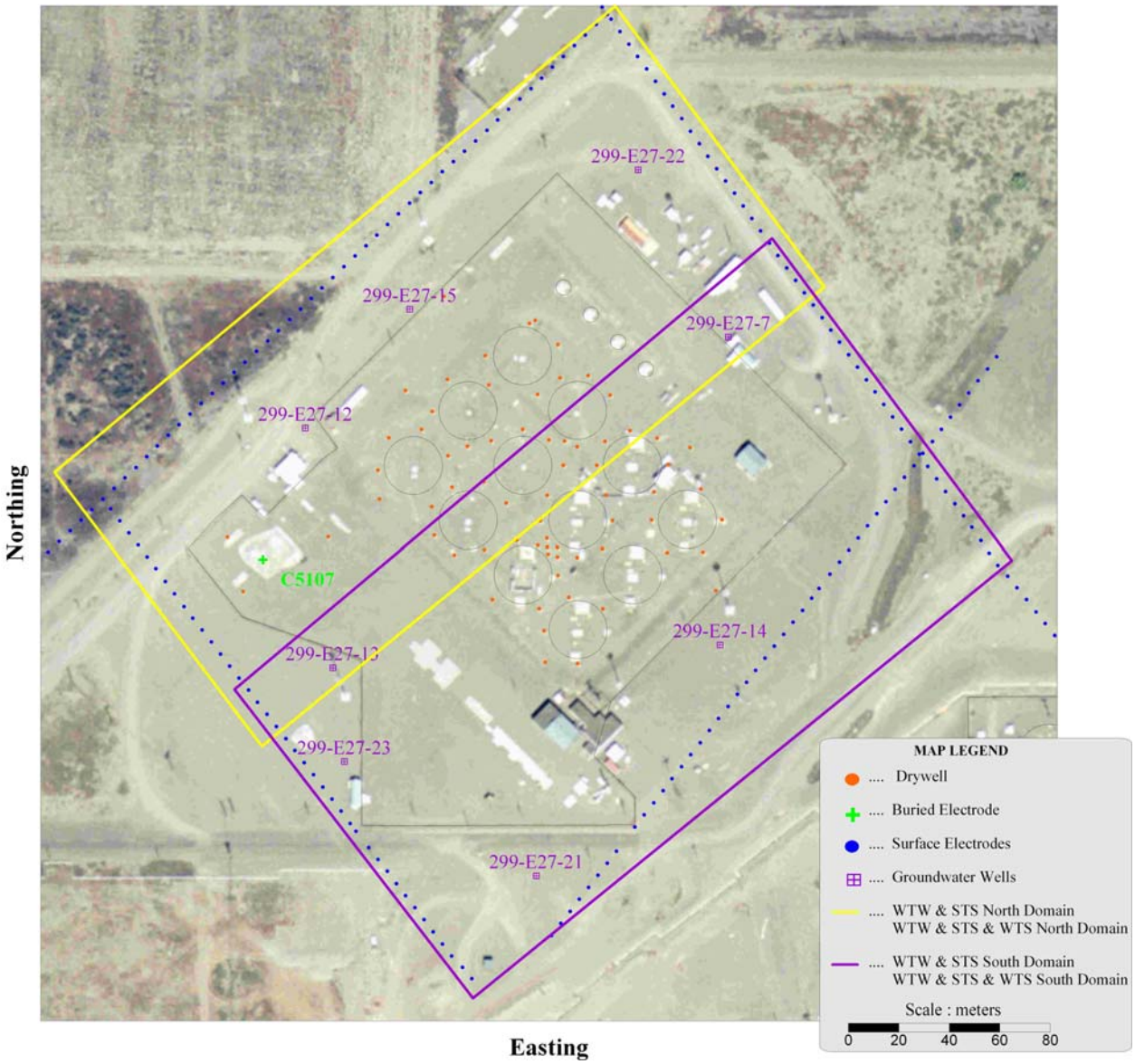

Table 6. Comparison of WTS Final Inversion Results for the Individual Modeling Domains.

Data Type	Model	Data Points Used	% of Data Population	Convergence			Data Range (ohm-meter)	
				Itera-tions	RMS	L2	Small	Big
WTW and STS	South	2,505	23	19	4.9	0.7	10.0	15.0
	North	3,254	30	11	9.1	2.7	N/A	N/A
WTW, WTS, and STS	South	7,035	26	20	5.9	1.4	N/A	N/A
	North	6,626	24	20	5.3	0.8	N/A	N/A

L2 = L2 Normalization.
N/A = Not applicable, data set was not plotted since convergence parameters were not acceptable.
RMS = root mean squared.
STS = surface-to-surface.
WTS = well-to-surface.
WTW = well-to-well.

5.0 CONCLUSIONS

Analysis of the resistivity data collected from the drywells in the WTW inversion produced results that met acceptance criteria in terms of statistical analysis of the inversion model results. Inversion of the WTW data identified low resistivity zones in the vicinity of tank C-104 and C-105 and a smaller zone just north of C-108. These results do not coincide with the confirmed or assumed tank leaks identified in the Waste Tank Summary Report (HNF-EP-0182), which does not show any recorded release events near the two low resistivity anomalies. However, the resistivity results are consistent with indications of a loss of waste fluids between tanks C-104 and C-105. Both the known cascade line leaks at this location and plausible C-105 tank leak are potential sources of vadose zone contamination contributing this anomalous resistivity zone. Analysis of the other data combinations did not produce results that met acceptance criteria in terms of statistical analysis of the model output and therefore instill a low level of confidence that the model output matches the field data.

Inversion modeling efforts were impacted due to computer software/hardware limitations. Inversion of all electrode combinations, with the exception of WTW drywell-only, produced a wide variety of resistivity anomaly maps. Agreement between the various combinations was poor and is likely the result of breaking the data into subsets. Data quality was acceptable and some agreement was observed for the WTW groundwater and drywell subsets. It is therefore expected that results could be improved if the data were re-inverted under a single domain. The current B farm SGE effort includes an upgrade of the EarthImager3D inversion software. The upgrade will allow the software to utilize a multi-CPU architecture and 16 times more memory. Under the new software, modeling efforts could be concentrated to one unified model that would contain all electrode data sets. The current inversion results could be used to control inversion parameters and will greatly reduce the number of iterations needed for acceptable data convergence.

Inversion modeling was further impacted by limitations in data coverage. Previous SGE deployments provided multiple surface electrode survey lines that were used to cross-validate individual responses and generate an even distribution of data points within the domain. The lack of surface electrode coverage for this deployment at C tank farm makes correlation of anomalous features to infrastructure or low-resistivity plumes nearly impossible. In addition, the great distance between the surface lines and the nearest drywells greatly decreased inversion modeling convergence parameters. Additional surface data within the boundary of the four perimeter lines would not increase the domain memory requirements because the modeling cells are already included as part of the perimeter domain. However, the additional data would improve data density which would help constrain individual resistivity anomalies within the inversion.

The WTW data had the lowest error, largely due to the high signal strength, and produced the lowest inversion model fitting error (RMS error). In contrast, the surface data, along the four individual resistivity lines, showed the highest error and coverage proved too limited in scope to compile a valid three-dimensional inversion. Interpretation of the two-dimensional results was unreliable due to high data error percentages that seemed to be caused by possible subsurface infrastructure and electrical noise. Two-dimensional inversion was useful as a quality control data filtering step to discriminate poor quality data before completing three-dimensional inversion using surface data (WTS and combinations).

It is difficult to evaluate the performance of the buried electrode, given the uncertainty of the individual inversion subset results. The single-depth electrode did not provide additional supporting data due to its placement, which was beyond the WTW modeling area, and the limited quantity of data provided by a single electrode. However, the installation of the electrode using a modified cone penetrometer tip appears to provide acceptable data. Transmitted current and received signal quality was better than a typical surface electrode, but not as good as a well electrode, which has a considerably larger grounding surface area. It is difficult to rate the performance of the electrode if no measured resistivity anomaly surrounds the buried electrode. WTW inversion results that included the buried electrode also showed no resistivity anomalies associated with the buried electrode. The data quality of the electrode suggests that a significant future value can be realized when additional buried electrodes are installed that could augment the limited geometry. Results from forward modeling, conducted as part of the T farm SGE project, showed a significant increase in vertical resolution when several depth electrodes are deployed in dispersed locations throughout the WTW modeling area. Work conducted for the B-Complex SGE effort utilizing several depth electrodes is expected to produce sufficient data for a field scale verification of forward modeling results.

6.0 LIMITATIONS

6.1 MODEL DOMAIN LIMITATIONS

The most detrimental limitation to modeling the resistivity data was the need to split the total data set into subsets to accommodate limited computational memory (RAM) issues. Although the computer's RAM was maximized to four gigabytes, the Windows XP operating system only makes two gigabytes accessible to the EarthImager3D software. A two-gigabyte memory allocation only allows the software to generate a domain of 5×10^5 finite difference cells. The number of cells in a model is determined by the expanse of the domain (i.e., the width, depth, and length of the domain as determined by the location of the farthest electrodes) and by the number of unique rows and columns used in the model. For example, a series of electrodes in a single row will require less unique cells, and therefore, less memory than a set of randomly placed electrodes. To reduce memory based on domain size issues, the domain was divided into smaller subsets with some electrode geometries requiring up to four sub-domains to capture all relevant aspects of the site assessment. Additionally, to help reduce the number of rows and columns in the domain for the C tank farm model, the coordinate system was rotated 39 degrees counterclockwise.

An example of the inconsistent inversion results from splitting the domain into smaller subsets is presented in the following figures. The focus of the discussion will be around the 241-CR-151 Diversion Box in the southern portion of the farm. This is near where unplanned release UPR-200-E-81 resulted in a release of approximately 36,000 gallons (136,000 liters) in 1969.

Six of the inversion domain subsets included the diversion box in the model domain including the WTW ('All Wells Central Domain' and 'All Wells South Domain'), WTS ('WTS South Domain' and 'WTS West Domain'), WTW&STS ('South Domain') and WTW&STS&WTS ('South Domain'). The results from each domain subset are presented as Figures 17 through 22, respectively.

Figure 17. Inversion Results for WTW 'All Wells Central Domain.'

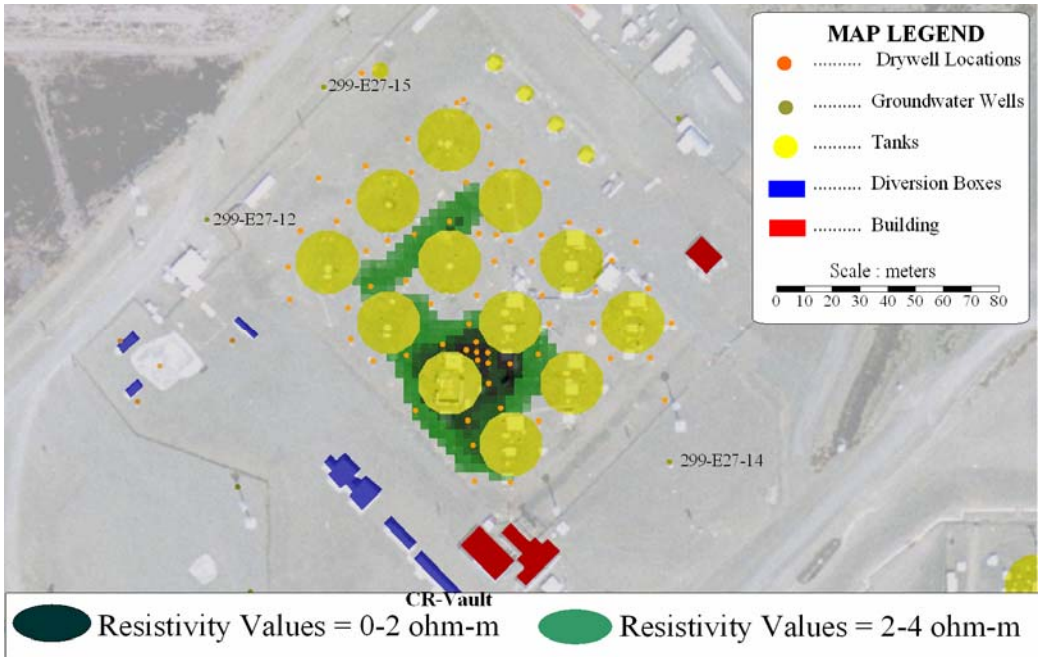

Figure 18. Inversion results for WTW 'All Wells South Domain.'

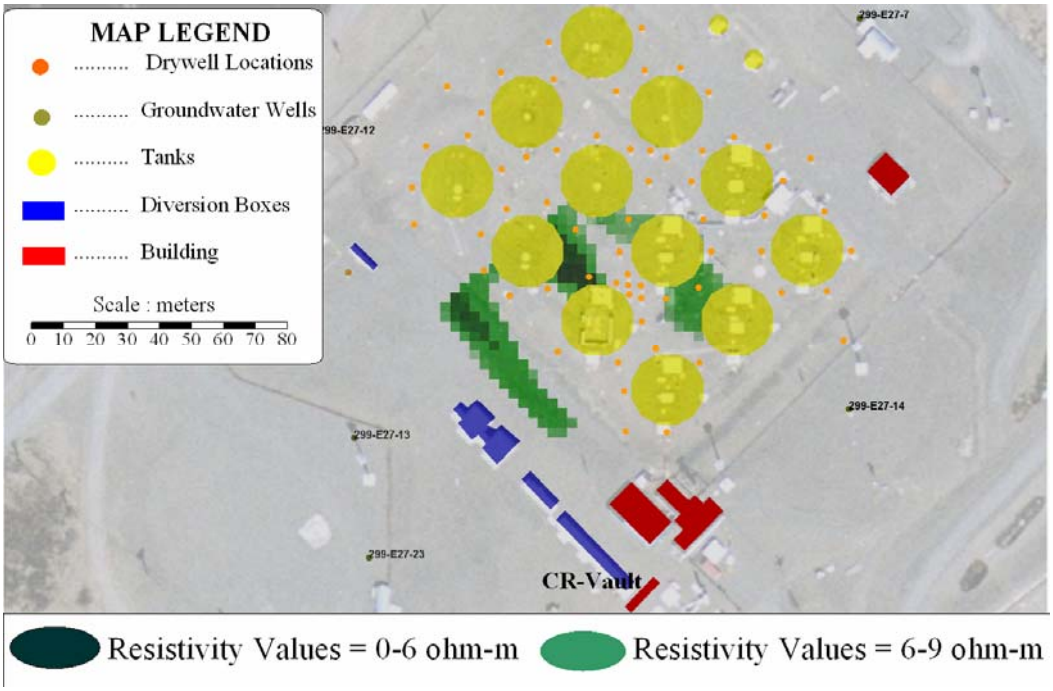

Figure 19. Inversion results for WTS 'South Domain.'

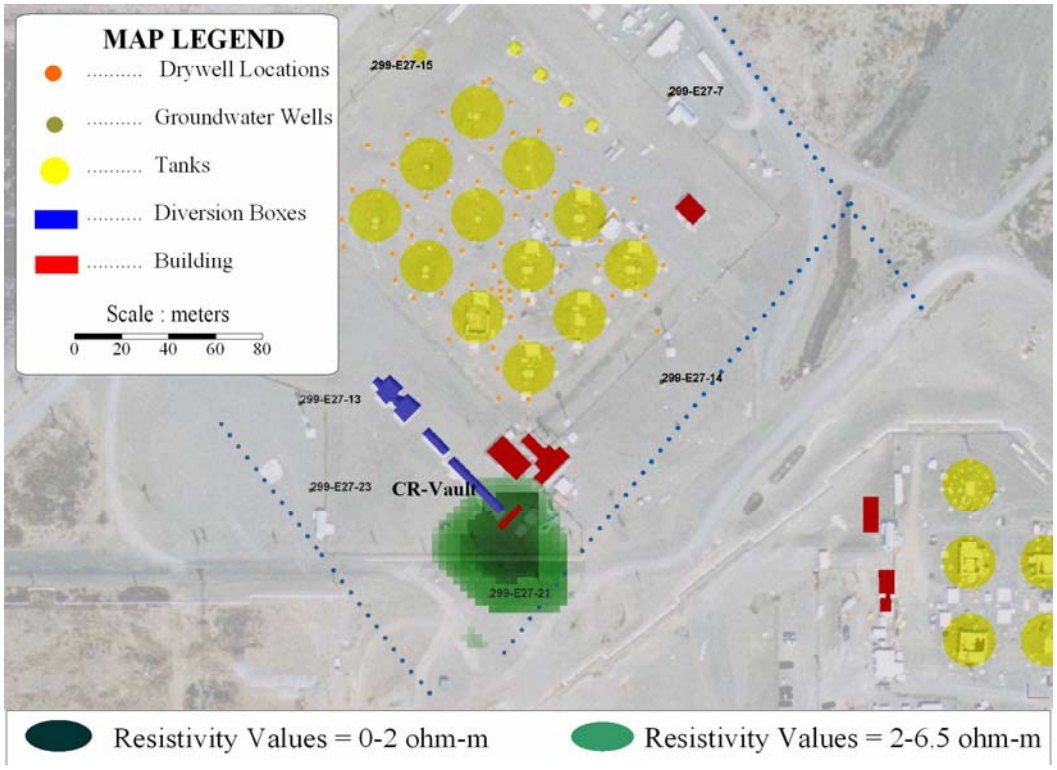

Figure 20. Inversion results for WTS 'West Domain.'

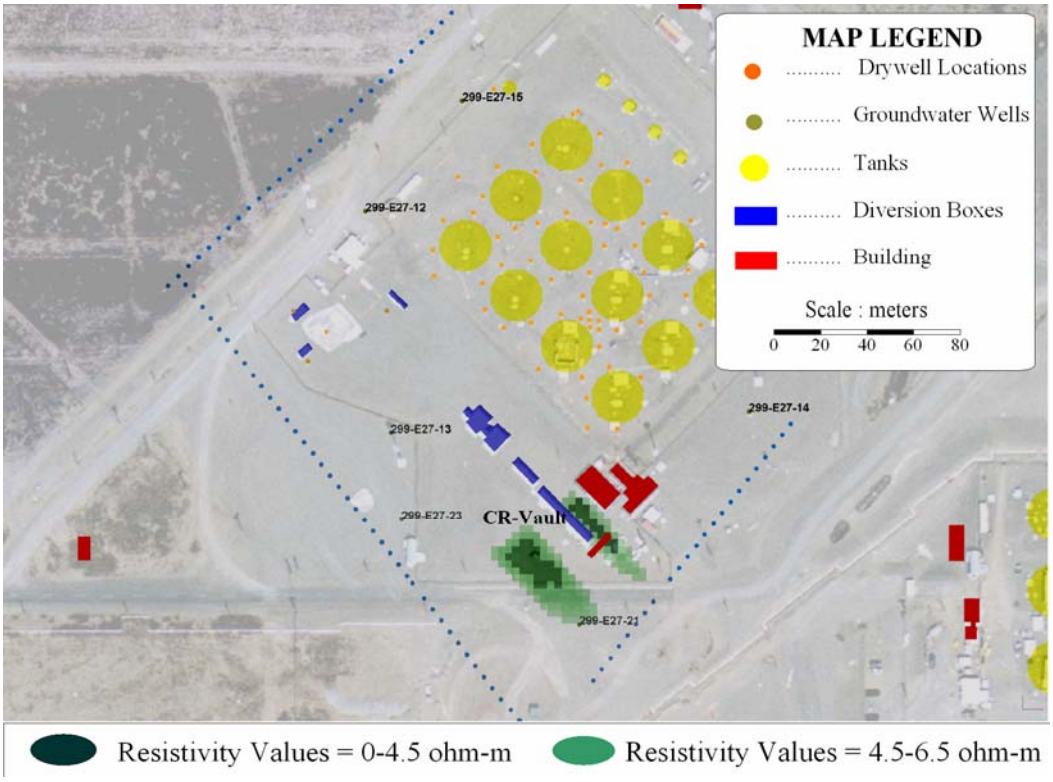

Figure 21. Inversion results for WTW&STS 'South Domain.'

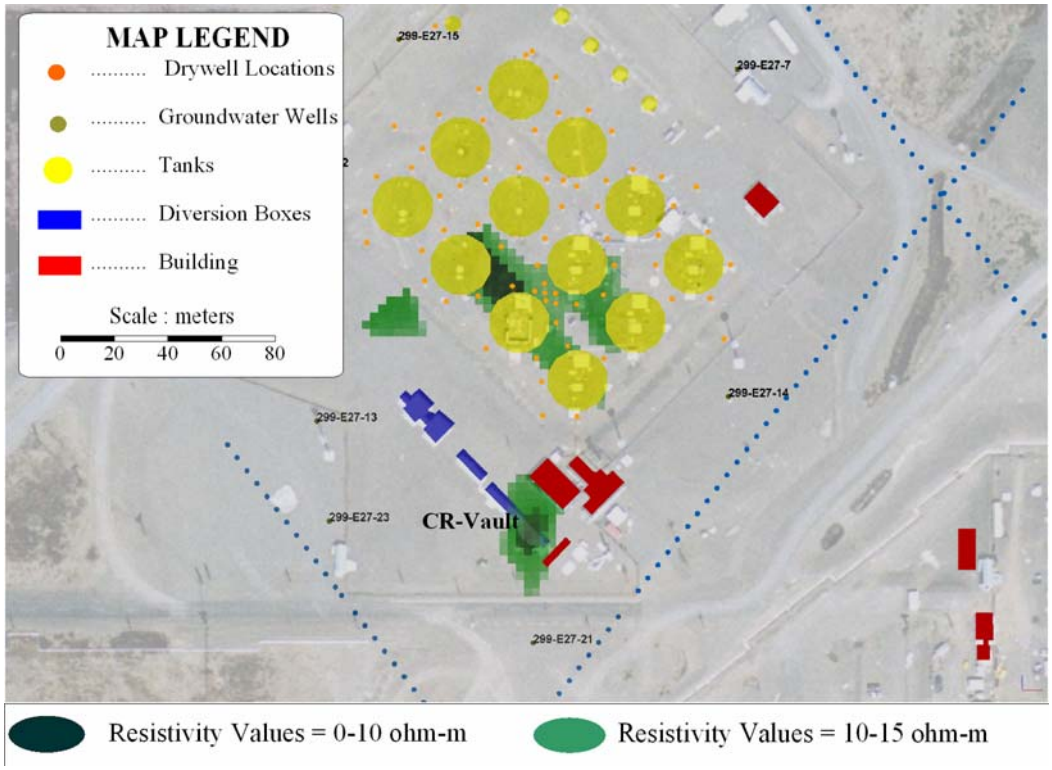

Figure 22. Inversion results for WTW&STS&WTS 'South Domain.'

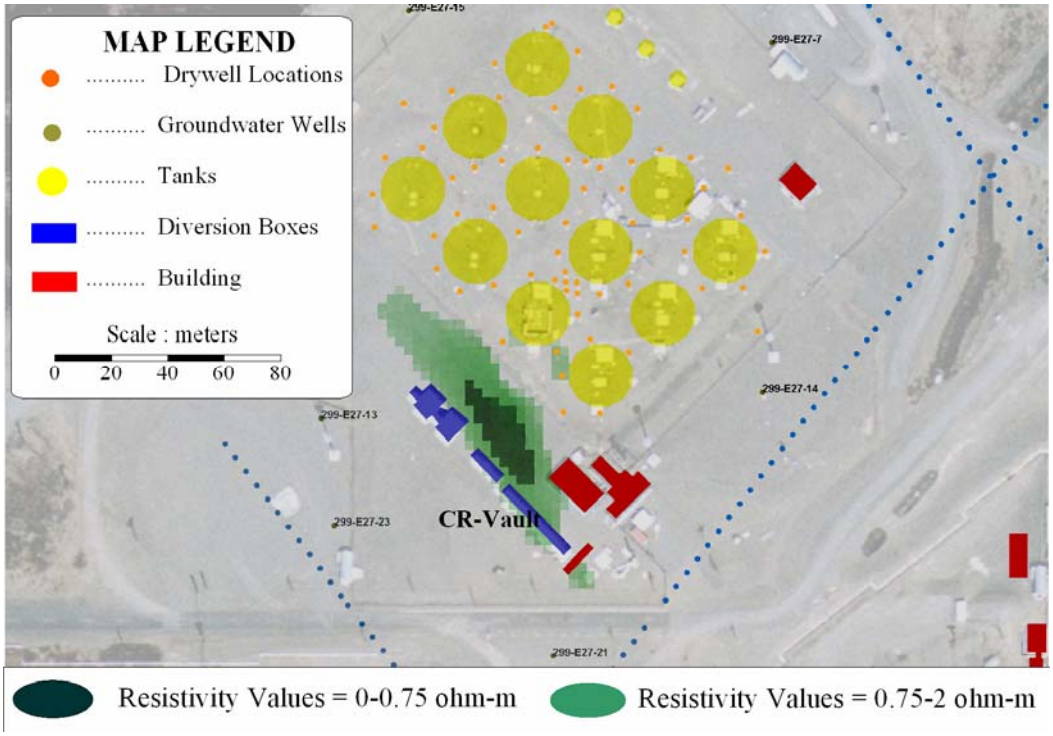

The results of the individual domain subsets in Figures 17 through 22 show different plume shapes and values. Firstly, for inversion models without surface electrodes, a low resistivity anomaly does not exist near the diversion box (Figure 17 and 18). For the remaining four models, the low resistivity anomaly is either round (Figure 19 and 21) or elongated (Figures 20 and 22). Additionally, the resistivity values representing the two plumes vary significantly within each figure. Based on these disparate results, low confidence is given to the shape and resistivity value of the anomaly. However, there is a high degree of corroboration among several figures as to the existence of an anomaly. It is not possible to interpret which of the competing results is valid without performing a joint inversion involving the complete data set.

6.2 ISSUES AND CONCERNS ASSOCIATED WITH INTERPRETATION

SGE inversion results show low-resistivity anomalies that may be caused by an increase in soil moisture or inorganic salt concentrations. Laboratory resistivity measurements of soil samples representative of the Hanford, Cold Creek and Ringold Formations are currently being acquired to derive petrophysical relations. It is hoped that quantified relationships between electrical resistivity in response to increasing water content and soil contaminants (e.g., sodium nitrate) content will allow better calibration of observed SGE resistivity anomalies. The resulting data should provide a better understanding of what resistivity levels, in ohm-meters, best represent actual plume boundaries.

It is important to consider the confidence and reliability of the inversion results in order to avoid false positives and false negatives. To help establish confidence in evaluating areas of low resistivity, the following criteria should be confirmed.

- Do the results match hydrologic expectations correlating to waste disposal areas?
- Can the results be verified through core sampling data?
- Can the results be verified through a different geometric configuration of SGE?
- Are the low-resistivity areas continuous over broad areas?

Direct comparisons should not be made to the other characterization methods employed at the tank farms, such as spectral gamma logging. This comparison is not endorsed on many levels. First, the scales of measurement between the two systems are highly disparate. The spectral gamma probe logs a drywell with a field of vision near the well. By contrast, SGE obtains large-scale volumetric averages covering areas the size of a tank farm. The scale increases for surface resistivity inversion with depth, and increases for WTW inversion at larger separations. Second, the contaminant of interest for each method (i.e., inorganic salts for SGE and gamma-emitting radionuclides for spectral gamma) moves through the vadose zone under different mechanisms. Inorganic salts, especially nitrate, are transported primarily under advection or diffusion with little to no retardation. The nitrate plume will be relatively large. Most gamma-emitting radionuclides have large retardation coefficients under natural conditions and are transported more slowly. These radionuclide plumes associated with the gamma-emitting radionuclides are expected to be much smaller than the inorganic salt plumes.

7.0 RECOMMENDATIONS

Several recommendations are suggested to improve the data acquisition, data quality, and data coverage of future SGE efforts at the Hanford Site tank farms.

1. It is strongly recommended that a full data set inversion be performed when the inversion software upgrade is completed. All inversion results, with the exception of WTW drywells only, suffered as a result of the inversion software and hardware limitations that forced operators to break data sets into smaller fractions of the total data population. The complexity and large spatial area of the C tank farm project site could not be adequately modeled using current inversion software and hardware. Results of the individual modeling domains suggest that good information could be achieved if all electrode data sets are inverted as a single model.

2. All inversion results that utilized surface data suffered as a result of the reduced electrode deployment, which consisted of four orthogonal lines surrounding the C tank farm perimeter. Inversion results for this SGE effort demonstrate that surface data are only valuable when deployed with sufficient resolution and geometry. Future SGE efforts should be deployed with sufficient line and electrode spacing to adequately resolve the spatial and vertical location of observed resistivity anomalies. At a minimum, surface electrodes should be deployed along equally spaced orthogonal lines.

3. If limited scope SGE deployments are performed, the investigation should be limited to WTW data collection.

4. Vertical resolution is relatively low (compared to lateral resolution) for the surface resistivity data collection and non-existent for WTW resistivity. It is recommended that future SGE deployments include as many subsurface point electrodes as possible that are located within the central monitoring well area. An additional enhancement would be to deploy several depth electrodes along each borehole in order to construct an electrical resistivity tomography array. Forward modeling discussed in RPP-RPT-28955 demonstrated a significant improvement in vertical resolution using depth electrode data.

5. Develop a strategy to increase confidence in the SGE results through confirmatory vadose zone sediment and pore water sampling analysis of key inorganic constituents (i.e., nitrate and nitrite) in the vadose zone.

8.0 REFERENCES

Agnew, S.F., 1993, *Analysis of the 241-C Farm*, LAUR-93-3605, Los Alamos National Laboratory, Los Alamos, New Mexico.

Agnew, S.F., 1997, *Hanford Tank Chemical and Radionuclide Inventories: HDW Model, Rev. 4*, LAUR-96-3860, Los Alamos National Laboratory, Los Alamos, New Mexico.

Brodeur, J.R., 1993, *Assessment of Unsaturated Zone Radionuclide Contamination Around Single-Shell Tanks 241-C-105 and 241-C-106*, WHC-SD-EN-TI-185, Westinghouse Hanford Company, Richland, Washington.

DOE/ORP-2003-11, 2003, *Preliminary Performance Assessment for Waste Management Area C at the Hanford Site, Washington*, Rev. 0, CH2M HILL Hanford Group, Inc., Richland, Washington.

DOE/ORP-2005-01, 2006, *Initial Single-Shell Tank System Performance Assessment for the Hanford Site*, Rev. 0 Draft, U.S. Department of Energy, Office of River Protection, Richland, Washington.

DOE/RL-89-28, 1993, *PUREX 216-B-3 Pond System Closure/Post Closure Plan*, Rev. 2, U.S. Department of Energy, Richland Operations Office, Richland, Washington.

GJO-97-1-TARA, 2000, *Hanford Tank Farms Vadose Zone: Addendum to the U Tank Farm Report*, GJO-HAN-8, U.S. Department of Energy, Grand Junction Office, Grand Junction, Colorado.

HNF-EP-0182, 2006, *Waste Tank Summary Report for Month Ending June 30, 2006*, Rev. 219, Lockheed Martin Hanford Corporation, Richland, Washington.

PNNL-15670, 2006, *Hanford Site Groundwater Monitoring for Fiscal Year 2005*, Pacific Northwest National Laboratory, Richland, Washington.

RPP-7494, 2001, *Historical Vadose Zone Contamination from A, AX, and C Tank Farm Operations*, Rev. 0, Prepared by Fluor Federal Services for CH2M HILL Hanford Group, Inc., Richland, Washington.

RPP-14430, 2003, *Subsurface Conditions Description of the C and A-AX Waste Management Areas*, Rev. 0, CH2M HILL Hanford Group, Inc., Richland, Washington.

RPP-15317, 2003, *241-C Waste Management Area Inventory Data Package*, Rev. 0, CH2M HIL Hanford Group, Inc., Richland, Washington.

RPP-16608, 2004, *Site-Specific Single-Shell Tank Phase 1 RCRA Facility Investigation/Corrective Measures Study Work Plan Addendum for Waste Management Areas C, A-X, and U*, Rev. 1, prepared by J.D. Crumpler, Columbia Energy & Environmental Services, Inc., for CH2M HILL Hanford Group, Inc., Richland, Washington.

RPP-23748, 2006, *Geology, Hydrogeology, Geochemistry, and Mineralogy Data Package for the Single-Shell Tank Waste Management Areas at the Hanford Site*, Rev. 0, CH2M HILL Hanford Group, Inc., Richland, Washington.

RPP-26744, 2005, *Hanford Soil Inventory Model, Rev. 1*, Rev. 0, CH2M HILL Hanford Group, Inc., Richland, Washington.

RPP-23405, 2004, *Tank Farm Vadose Zone Contamination: Volume Estimates for Risk Assessments*, Rev. 0, CH2M HILL Hanford Group, Inc., Richland, Washington.

RPP-RPT-28955, 2006, *Surface Geophysical Exploration of T Tank Farm*, Rev. 0, CH2M HILL Hanford Group, Inc., Richland, Washington.

RPP-RPT-30976, 2006, *Surface Geophysical Exploration of S Tank Farm at the Hanford Site*, Rev. 0, CH2M HILL Hanford Group, Inc., Richland, Washington.

RPP-RPT-31557, 2006, *Surface Geophysical Exploration of U Tank Farm at the Hanford Site*, Rev. 0, CH2M HILL Hanford Group, Inc., Richland, Washington.

APPENDIX A

C TANK FARM SURFACE GEOPHYSICAL EXPLORATION FIGURES

Figure A-1. High Resolution Resistivity at the 241-C Farm.

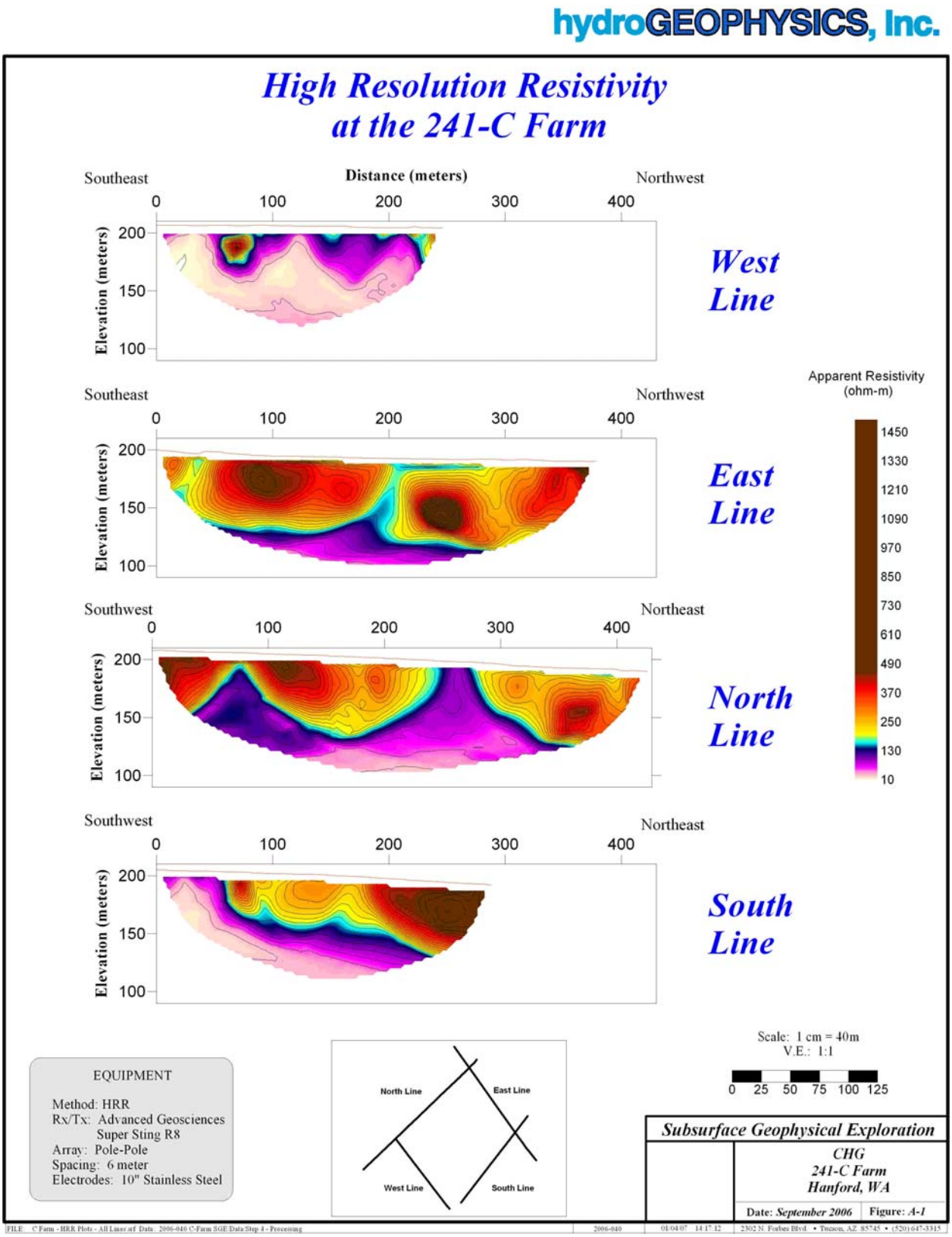

Figure A-2. 2D Inversions at the 241-C Farm.

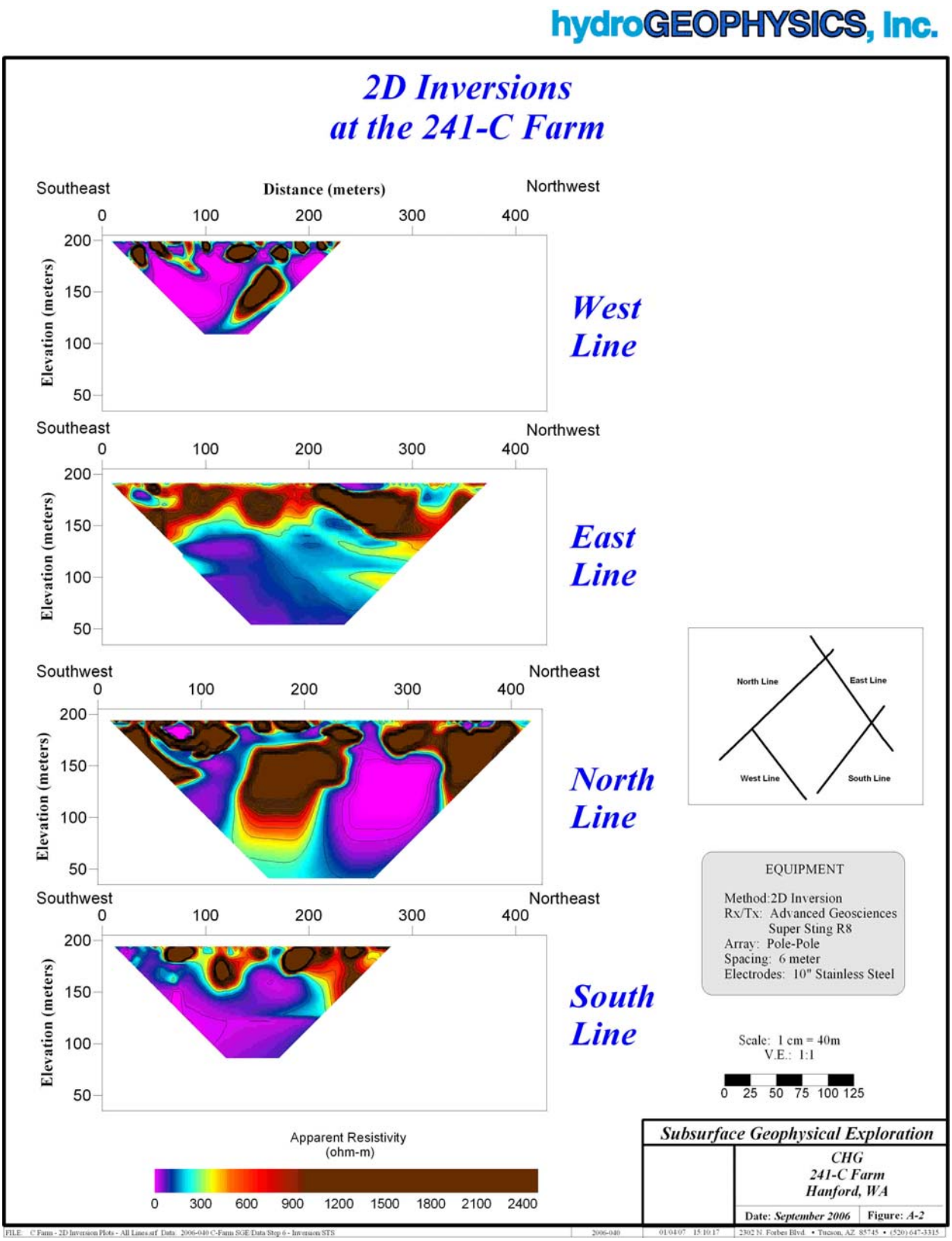

Figure A-3. High Resolution Resistivity and 2D Inversion at the 241- Farm - West Line.

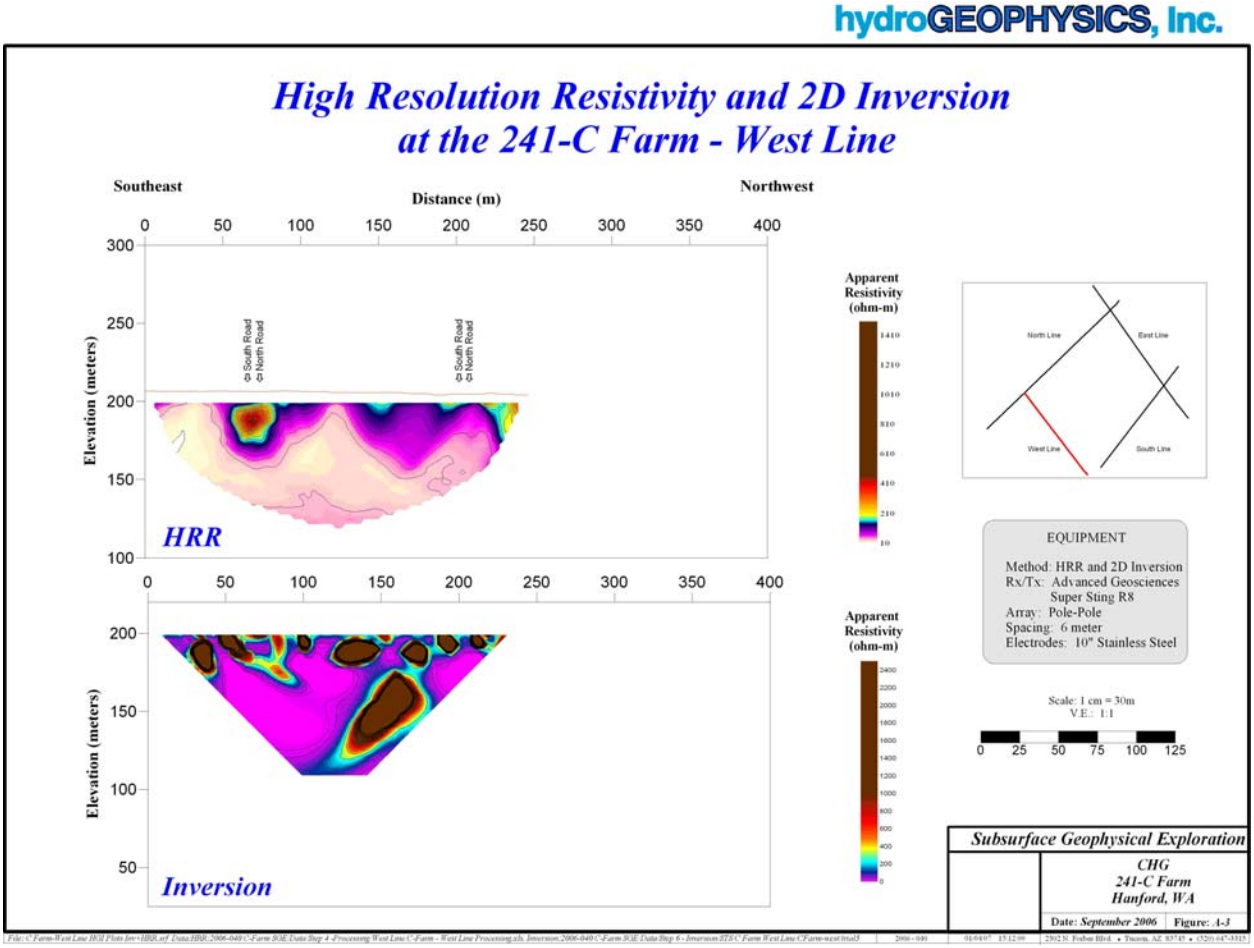

Figure A-4. High Resolution Resistivity and 2D Inversion at the 241-C Farm - East Line.

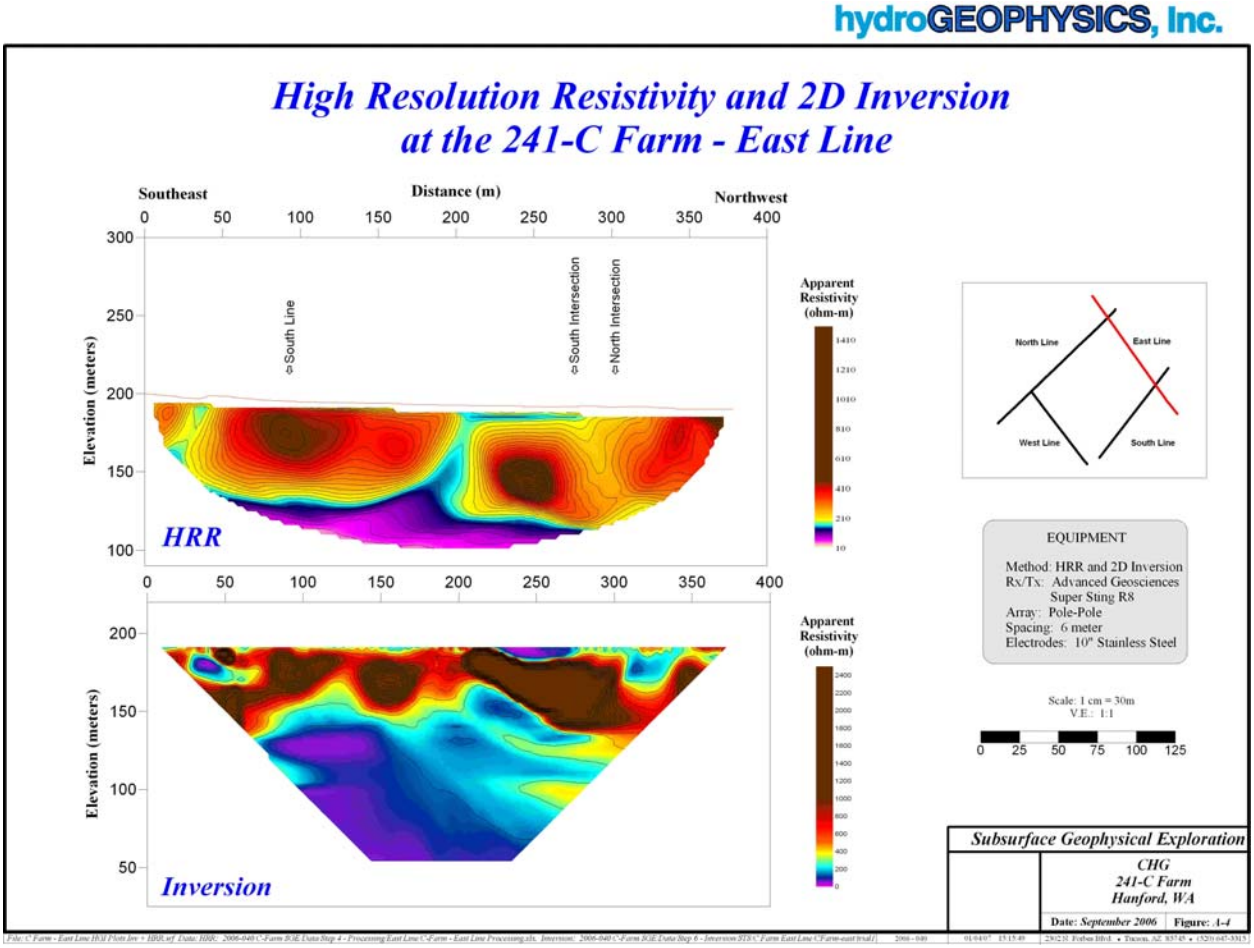

Figure A-5. High Resolution Resistivity and 2D Inversion at the 241-C Farm - South Line.

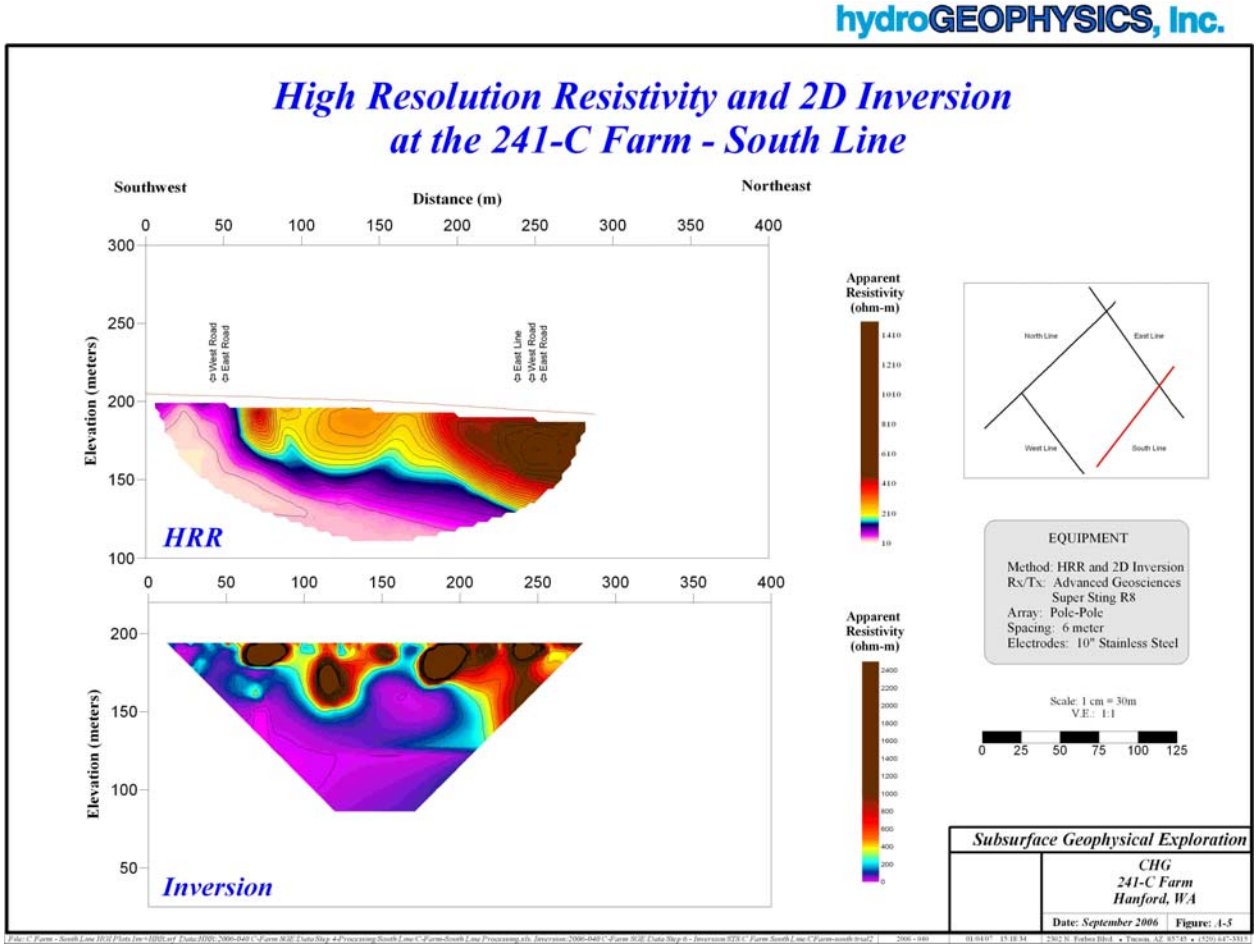
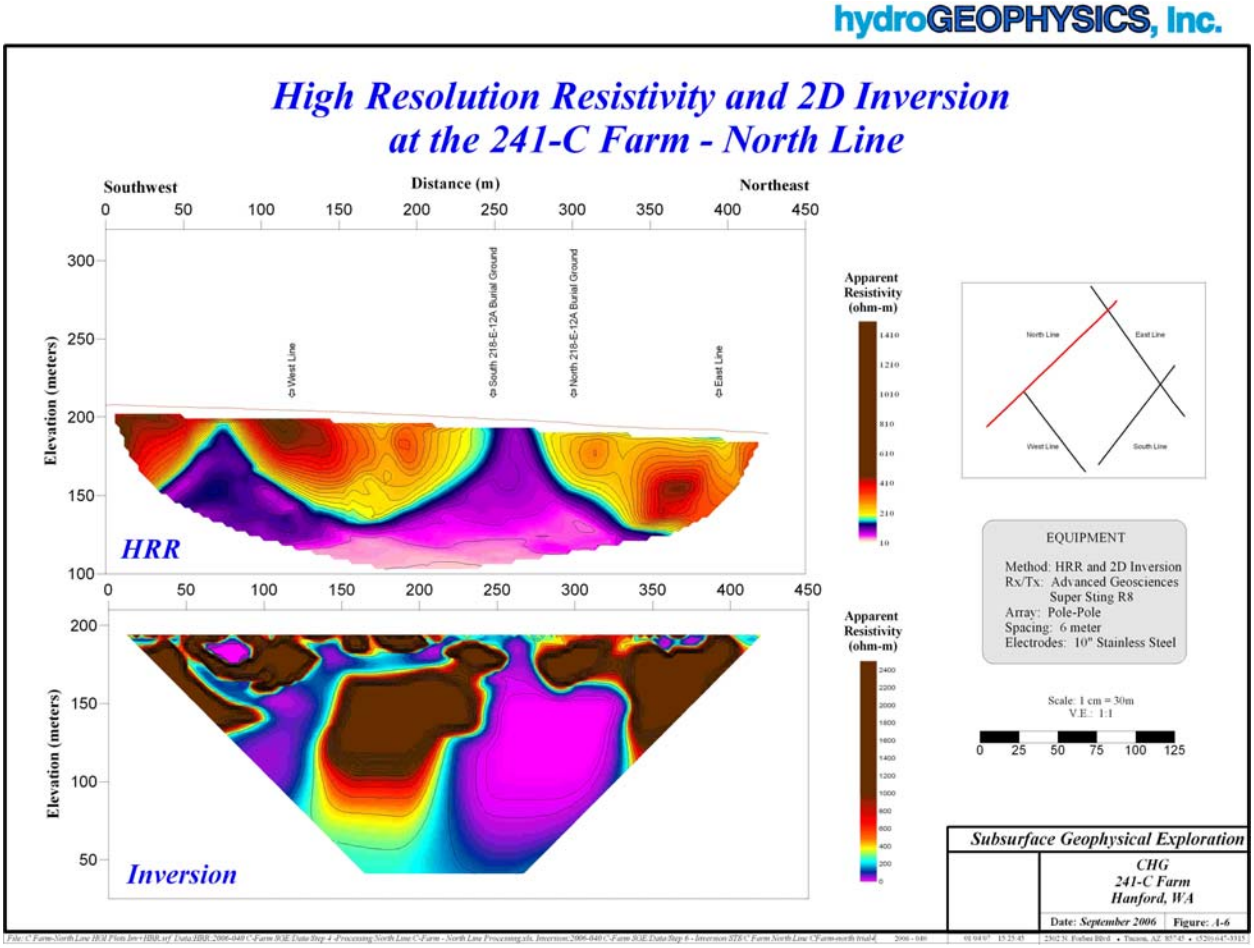
Figure A-6. High Resolution Resistivity and 2D Inversion at the 241-C Farm - North Line.